# Dissolved organic carbon, major and trace elements in peat pore water of sporadic, discontinuous and continuous permafrost zone of Western Siberia

Tatiana V. Raudina[1], Sergey V. Loiko[1], Artyom G. Lim[1], Ivan V. Krickov[1], Liudmila S. Shirokova[2,3], Georgy I. Istigechev[1], Daria M. Kuzmina[1], Sergey P. Kulizhsky[1], Sergey N. Vorobyev[1], Oleg S. Pokrovsky[2]*

[1] BIO-GEO-CLIM Laboratory, Tomsk State University, Lenina av., 36, Tomsk, Russia
[2] Geoscience and Environment Toulouse, UMR 5563 CNRS University of Toulouse (France), 14 Avenue Edouard Belin, 31400 Toulouse, France
[3] N. Laverov Federal Center for Integrated Arctic Research, Russian Academy of Science, Arkhangelsk, Russia

*Correspondence to*: Oleg S. Pokrovsky (oleg.pokrovsky@get.omp.eu)

**Abstract.** Mobilization of dissolved organic carbon (DOC) and related trace elements (TE) from the frozen peat to surface waters in the permafrost zone is expected to enhance under on-going permafrost thaw and active layer thickness (ALT) deepening in high latitude regions. The interstitial soil solutions are efficient tracers of on-going bio-geochemical processes in the critical zone and can help to decipher the intensity of carbon and metals migration from the soil to the rivers and further to the ocean. To this end, we collected, across a 640-km latitudinal transect of sporadic to continuous permafrost zone of western Siberia peatlands, soil porewaters from 30-cm depth using suction cups and we analyzed DOC, DIC and 40 major and TE in 0.45-µm filtered fraction of 80 soil porewaters.

Despite an expected decrease of the intensity of DOC and TE mobilization from the soil and vegetation litter to the interstitial fluids with the increase of the permafrost coverage, decrease in the annual temperature and ALT, the DOC and many major and trace element did not exhibit any distinct decrease in concentration along the latitudinal transect from 62.2°N to 67.4°N. The DOC demonstrated a maximum of concentration at 66°N, on the border of discontinuous/continuous permafrost zone, whereas the DOC concentration in peat soil solutions from continuous permafrost zone was equal or higher than that in sporadic/discontinuous permafrost zone. Moreover, a number of major (Ca, Mg) and trace (Al, Ti, Sr, Ga, rare earth elements (REEs), Zr, Hf, Th) elements exhibited an increasing, not decreasing northward concentration trend. We hypothesize that the effect of temperature and thickness of the ALT are of secondary importance relative to the leaching capacity of peat which is in turn controlled by the water saturation of the peat core. The water residence time in peat pores also plays a role in enriching the fluids in some elements: the DOC, V, Cu, Pb, REE, Th were a factor of 1.5 to 2.0 higher in mounds relative to hollows. As such, it is possible that the time of reaction between the peat and downward infiltrating waters essentially controls the degree of peat pore-water enrichments in DOC and other solutes. A two-degree northward shift in the position of the permafrost boundaries may bring about a factor of 1.3 ± 0.2 decrease in Ca, Mg, Sr, Al, Fe, Ti, Mn, Ni, Co, V, Zr, Hf, Th and REE porewater concentration in continuous and discontinuous permafrost zones, and a possible decrease in DOC, SUVA, Ca, Mg, Fe and Sr will not exceed 20% of their current values. The projected increase of ALT and vegetation density, northward migration of the permafrost boundary, or the change of hydrological regime are unlikely to modify chemical composition of peat pore water fluids larger than their natural variations within different micro-landscapes, i.e., within a factor of 2. The decrease of DOC and metal delivery to small rivers and lakes by peat soil leachate may also decrease the overall

export of dissolved components from continuous permafrost zone to the Arctic Ocean. This challenges the current paradigm on the increase of DOC export from the land to the ocean under climate warming in high latitudes.

## 1 Introduction

Boreal and subarctic regions of the Northern Hemisphere are among the most vulnerable areas to on-going climate warming (Natali et al., 2011, 2015; Schuur et al., 2015; Vonk et al., 2015b; Pries et al., 2016). Because of sizeable carbon storage in frozen soils of Siberia (Botch et al., 1995; Krementski et al., 2003; Frey and Smith, 2007; Beilman et al., 2009; Tarnocai et al., 2009; Gentsch et al., 2015), the warming in this region is especially important for global projections of the carbon balance on the planet (Smith et al., 2004; Frey and Smith, 2005; Feng et al., 2013). In this regard, permafrost-bearing part of Western Siberia Lowland (WSL) is highly sensitive to soil warming, due to (*i*) the dominance of discontinuous, sporadic and intermittent permafrost coverage compared to continuous and discontinuous permafrost of central and eastern Siberia and Canada High Arctic; (*ii*) the surface layer temperature of the WSL permafrost is often between 0 and -2°C, which is warmer than in other regions of the world (Romanovsky et al., 2010); (*iii*) essentially flat area of the WSL and high impact of flooding and thermokarst development, and most importantly (*iv*) high stock of ancient and recent organic carbon in the form of partially frozen peat deposits of 1 to 4 m thickness.

Mobilization of dissolved organic and inorganic carbon (DOC and DIC, respectively) and related trace elements (TE) including metal contaminants and micronutrients from the frozen peat to surface waters and further to the Arctic Ocean is one the major consequences of on-going permafrost thaw (Tank et al., 2012a, b, 2016; Striegl et al., 2005; Rember and Trefry, 2004; Prokushkin et al., 2011; Mann et al., 2012; Grosse et al., 2016; Holmes et al., 2013). The impact of warming on arctic and subarctic soil is primarily through the active layer thickness (ALT) rise (Zhang et al., 2005; Akerman and Johannson, 2008) although a number of other phenomena (plant productivity, drainage and hydrological regime change, ground fires etc) may be even more important in changing the biogeochemical cycle of carbon and metals in permafrost-affected soils (Jorgenson et al., 2013). For these reasons, the peat land zones have received significant attention (Haapalehto et al., 2011; Olefeldt and Roulet, 2012; Charman et al., 2013; Quinton and Baltzer, 2013; Muller et al., 2015; Morison et al., 2017), notably via natural manipulation experiments in order to assess the responses of peat carbon to simulated warming and oxidizing (Dielman et al., 2016; Liu et al., 2016), water table manipulation (Blodau and Moore, 2003; Strack et al., 2008; Goldberg et al., 2010) and drought (Clark et al., 2012).

The majority of available studies adressed the carbon and element transformation in the permafrost regions via analysis of rivers (Lobbes et al., 2000; Striegl et al., 2005; Spencer et al., 2008, 2015; Holmes et al., 2012; Wickland et al., 2012; Giesler et al., 2014; Mann et al., 2015), lakes (Kokelj et al., 2005, 2009; Guo et al., 2007; Laurion et al., 2010; Tank et al., 2009), mires (Olefeldt and Roulet, 2012; Olefeldt et al., 2013, 2014) or soil organic matter (SOM) from various depth and soil aqueous leachate (Swindles et al., 2015; Hodgkins et al., 2014, 2016; Drake et al., 2015; Vonk et al., 2015a; Yang et al., 2016) and largely ignored soil porewater chemistry. At the same time, interstitial soil solutions are known to be efficient tracers of on-going bio-geochemical processes in the critical zone (Hendershot et al., 1992; Stutter and Billett, 2003; Quinton and Pomeroy, 2006; Karavanova and Malinina, 2007; Gangloff et al., 2016) and can help to decipher the intensity of carbon and metals migration from the soil to the rivers and further to the ocean. However, in contrast to significant number of in-situ measurements of DOC and metals in the interstitial soil solutions of the boreal zone (Van Hees et al., 2000a, b; Reynolds et al., 2004; Starr and Ukonmaanaho, 2004; Michalzik et al., 2001; Giesler et al., 2006; Ilina et al., 2014; Griffiths and Sebestyen, 2016; Shotyk et al., 2016) there are relatively few studies of soil porewaters from the permafrost regions (e.g., Marlin et al., 1993; Prokushkin et al., 2005; Pokrovsky et al., 2006, 2013;

Koch et al., 2013; Jessen et al., 2014; Fouche et al., 2014; Fouché et al., 2014; Mavromatis et al., 2014; Herndon et al., 2015), none of them dealing with organic-rich peatland soils. Only recently, Frey et al. (2016) reported results soil pore waters from the yedoma wetland soil within the flow-path continuum from the soil to the Kolyma River mainstream.

In this work we sampled, across a 640-km latitudinal transect of sporadic to continuous permafrost, the interstitial soil solutions of the largest peatland of the world. Our main goal was to quantify the distribution of DOC, major and TE in pore waters along a permafrost gradient of similar micro-landscapes. Within the upper unfrozen peat horizon, we hypothesize a trend of diminishing DOC and metal concentration northward, due to the decrease of mean annual temperature, vegetation density and active layer thickness. We aimed at quantifying the latitudinal trend of peat pore water concentration of DOC, major and TE and testing the difference in solute concentration sampled from various micro-landscape such as mound, hollow, depression, and polygon. Implying a substituting-space-for-time approach, developed for surface waters of western Siberia, (i.e., Frey et al., 2007a, b; Frey and Smith, 2005), the obtained results should allow a straightforward empirical provisions of soil water chemistry change during northward migration of the permafrost boundary. Because the main source to inland waters in this vast territory (over 1 million km$^2$) occurs as supra-permafrost flow over the impermeable frozen peat horizon (Novikov et al., 2009), and due to the fact that the West Siberian peatlands contain the largest soil water and ice resources in the northern hemisphere (Smith et al., 2012), the assessment of soil peat water chemical composition should help predicting the possible change of DOC and metal transport of permafrost-bearing Siberian rivers and lakes under climate warming scenarios.

## 2. Materials and Methods

### 2.1. Geographical setting and local micro-landcapes

Western Siberia Lowland (WSL) includes the watershed of the Ob, Pur, Nadym, Poluy and Taz rivers that drain Pleistocene sands and clays, covered by thick (1 to 3 m) peat. All three major zones of the boreal biome, taiga, forest-tundra and tundra, can be found in this region. The territory investigated in this work includes 3 main permafrost zones: sporadic, discontinuous and continuous (Fig. 1). Quaternary clays, sands, and alevrolites underlying the surface peat deposits range in thickness from several meters to 200-250 m and have fluvio-glacial and lake-glacial origin in the north of 60°N. The climate is humid semi-continental with mean annual temperature (MAT) ranging from - 2.8°C in the south of the cryolithozone (Syrgut region) to -9.1°C in the north (Tazovsky). The annual precipitation ranges from 600 mm in Kogalym to 360 mm in Tazovsky. Along the gradient of discontinuous to sporadic to continuous permafrost zone, we selected 5 main test sites whose physico-geographical characteristics are given in **Table 1.**

A typical feature of the WSL is the presence of positive and negative forms of relief – microlandscapes. The initial bog with weakly pronounced micro-relief was subjected to freezing during Subboreal period (~ 4500 y.a). During Subatlantic period (2500 y.a.) and the increase of temperature and precipitation, the thermokarst started. The hollows received sufficient water and they started to thaw, whereas the mounds were rising due to ice wedges underneath (Panova et al., 2010; Ponomareva et al., 2012; Pastukhov et al., 2016). The positive forms include ridges in permafrost-free and sporadic permafrost zone, mounds in discontinuous permafrost zones, and polygons in the subarctic tundra of continuous permafrost. The negative forms comprise hollows (abundant across all zones), permafrost subsidences in discontinuous and continuous permafrost zones, and frost cracks of the polygonal tundra biome. In each of five major sites, several micro-landscapes corresponding to one positive and two negative form of relief were selected as specified in **Table 1** and shown as aerial views in **Fig. 1.** The cross sections of dominant micro-landscapes with corresponding soil specifications

are represented in **Fig. 2** and include: (*i*) peat mounds in the 4 southern sites of flat mound peat bog, and corresponding polygon in the most northern, Tazovsky site of polygonal tundra; (*ii*) hollows in all 5 sites, and (*iii*) permafrost subsidences in 4 southern sites and corresponding frost crack in Tazovsky. Typical soil profiles of studied sites are illustrated in **Fig. S1** of Supplement.

### 2.2. Soil porewater sampling

Altogether, 80 soil porous waters in 5 main sampling sites were collected in the end of July-beginning of August 2015. In this study, suction cup lysimeters were used. The chemical composition of interstitial soil solution is known to depend on the extraction method (e.g., Geibe et al., 2006; Schlotter et al., 2012). Detailed comparison between suction cup and press technique is described in methodological work of our group (Raudina et al., 2016). In the peat profile of each microlandscape, the PTFE suction cup lysimeters (95 mm long and 21 mm diameter, 2 µm pore size) of SDEC (France) were installed at the depth of 30±15 cm below the moss layer (**Fig. S2** of Supplement). The choice of the sampling depth was determined by the position of the permafrost table: typically, the cup was installed at 10 cm from the peat outcrop vertical surface, 5-10 cm above the bottom of the active layer, but not deeper than 40-50 cm from the moss layer. In all sites, the cups were installed exclusively in soils that belonged to group Histosols (according to WRB 2014, i.e., having a thickness of peat > 60 cm). The cups were connected via PTFE tubing to polypropylene 1-L container maintained at 75 to 50 kPa via a Mityvac MV8255 PVC-made hand pump or a portable electric vacuum pump (KNF Neuberger W/VAC. 5.5 L). Before each installation, the suction cups were cleaned by flushing with Milli-Q water (~ 250 mL), followed by 3% ultrapure HNO3 (~ 250 mL) and finally Milli-Q water (~ 750 mL). Each cup was soaked in Milli-Q water for at least 1 day before the experiment and was used only once. The porewater was collected in two steps. The first portion (100-200 mL) was collected during 24 h and the fluid was discarded, allowing for the saturation of the tubing and the recipient bottle surface. The 2$^{nd}$ portion (100-300 mL) was collected during the next 24 h of deployment or, in case of dryer conditions, over 48 h and used for analyses. The vacuum in the recipient bottle decreased from 75 kPa to atmospheric pressure over 24 h, and the first portion of the fluid appeared at 45 to 50 kPa.

### 2.3. Analyses

Collected waters were immediately filtered in pre-washed 30-mL PP Nalgene® flacons through single-use Minisart filter units (Sartorius, acetate cellulose filter) having a diameter of 25 mm and a pore size of 0.45 µm. The first 20 mL of filtrate were discarded. Filtered solutions for cation analyses were acidified (pH ~ 2) with ultrapure double-distilled $HNO_3$ and stored in pre-washed HDPE bottles. The preparation of bottles for sample storage was performed in a clean bench room (ISO A 10,000). Blanks were performed to control the level of pollution induced by sampling and filtration. The DOC blanks of MilliQ filtrate never exceeded 0.1 mg/L which is quite low for the organic-rich pore waters sampled in this study (i.e., 10–100 mg/L DOC). pH was measured in the field using a combined electrode with un uncertainty of ±0.02 pH units. DOC and DIC were analyzed using a Carbon Total Analyzer (Shimadzu TOC VSCN) with an uncertainty better than 3%. The instrument was calibrated for analysis of both form of dissolved carbon in organic-rich, DIC-poor waters (e.g., Prokushkin et al., 2011). The UV absorbance of the filtered samples was measured at 280 nm using quartz 10-mm cuvette on Cary-50 spectrophotometer. The specific UV-absorbency ($SUVA_{280}$, L $mg^{-1}$ $m^{-1}$) is used as a proxy for aromatic C, molecular weight and source of DOM (Uyguner and Bekbolet, 2005; Weishaar et al., 2003; Ilina et al., 2014 and references therein). The $SUVA_{280}$ in the present study was used for consistency with previous

measurements of lakes and rivers in western Siberia (Shirokova et al., 2013; Manasypov et al., 2015, 2017; Pokrovsky et al., 2015) and permafrost-draining rivers in Central Siberia (Prokushkin et al., 2011).

Major anions ($Cl^-$, $SO_4^{2-}$) concentrations were measured by ion chromatography (HPLC, Dionex ICS 2000) with an uncertainty of 2%. Major cations (Ca, Mg, Na, K), Si and ~40 TE were determined with an ICP-MS Agilent ce 7500 with In and Re as internal standards and 3 various external standards, placed each 10 samples in a series of river water. Details of TE analyses in DOC-rich waters of western Siberia are given elsewhere (Pokrovsky et al., 2016a, b). The SLRS-5 (Riverine Water Reference Material for Trace Metals certified by the National Research Council of Canada) was used to check the accuracy and reproducibility of each analysis (Yeghicheyan et al., 2013). Only the elements that exhibited good agreement between replicated measurements of SLRS-5 and the certified values (relative difference < 15%) are reported in this study.

### 2.4. Statistical treatment

The concentrations of carbon and major elements in soil porewaters were treated using the least squares method and Pearson correlation (SigmaPlot version 11.0/Systat Software, Inc). Regressions and power functions were used to examine the relationships between the elemental concentrations and the latitude of sampling. The normality of data distribution was checked using the criterion of Kolmogorov-Smirnov, separately for each site and for the full set of the data. The significance value was < 0.01 and thus non-parametric criteria for data comparison were used. First, major and TE concentrations in soil porewaters of (1) five main sampling sites and (2) four main micro-relief landscapes (polygon, permafrost/subsidence, frost crack and hollow) were processed using non-parametric H-criterion Kruskal–Wallis test. This test is suitable for evaluation of difference of each component among several samplings simultaneously. It is considered statistically significant at $p < 0.05$. In case of significant differences, a comparison of DOC, major and TE concentration between soil porewaters sampled in 3 main pair micro-landscapes (mound-hollow, mound-subsidence, and hollow-subsidence) of each 5 major sampling site was conducted using non-parametric pair Wilcoxon-Mann Whitney test. All graphics were performed using MS Excel 2010 and GS Grapher 11 package. Principal component analysis (PCA) was used for the full set of sampled soil porewaters across the micro-landscapes and permafrost zones. In this treatment, the main numerical variables were the geographic latitude of the sampling site, the depth of peat horizon, ALT, specific conductivity, pH, DOC, DIC, Cl, $SO_4$, Si, all major cations and 43 TE concentration.

The PCA analysis allowed to test the influence of various parameters, notably the latitude and the ALT on the soil porewater DOC and element variability. All the variables were normalized as necessary in standard package of STATISTICA-7 (http://www.statsoft.com) given that the units of measurements of various components are different. The identification of factors was performed using the method of Raw Data and the extraction method was principal component. The scree test involved plotting the eigenvalues in descending order of their magnitude against their factor numbers and determining where they level off. The PCA values demonstrated significant decrease of the value between F2 and F3 suggesting therefore that at least two factors are interpretable.

## 3. Results

### 3.1. PCA analysis and correlations between elements

The PCA analysis of all micro-landscapes and geographical zones yielded 2 possible factors contributing to observed variations in element concentration (i.e., 20 and 9%, **Fig S3 (A, B)** of Supplement). Such relatively low

proportion of the variance explained by PCA is consistent with previous treatments of the WSL river water, conducted on a much larger dataset (Pokrovsky et al., 2016a). Because the standard STATISTICA-7 package used in this work does not allow realization of Kaiser-Meyer-Olkin (KMO) criterion, we computed this criterion using Excel®. The KMO value was equal to 0.533 which suggests rather low adequacy: the analysis does not make sense at KMO < 0.5. Note that the removal a part of the data series and conducting separate PCA for major elements, TE, various forms of micro-relief and various geographical sites did not yield any better description of the variance mainly because of insufficient size of the dataset.

The first factor explains a greater variance in heavy element hydrolysates such as REEs, Cr, Nb, Zr, Hf, Th and U whereas the second factor was pronounced for soluble and biogenic elements (Mn, Co, Ni, V, Si, Ca, Mg, Sr), pH and latitude but also included Al and Fe, presumably due to organic complexation (see section 4.2 below). The correlation matrix (**Table S1** of Supplement) and respective dendrogram of a hierarchical cluster for scaled pore water score variation (**Fig. S3 C**) demonstrated pronounced link of Si with REEs, Zr, Nb, Fe, Cr, V and Li, probably corresponding to the source of these elements from silicate matrix of the peat profile. There was positive correlation between Mn and Ca and Sr and Ca, reflecting the biological impact or soluble carbonate minerals as it is established for riverwater of the region (Pokrovsky et al., 2016a). Note that the correlations of latitude, specific conductivity, pH and DOC with all major and TE were poorly pronounced (R < 0.5), whereas Fe and Al correlated with Si, Ti, V, Cr, Co, Ni, As, Zr, heavy REE, Hf.

### 3.2. Effect of micro-landscape

The mean values with S.D. of all major and TE in soil porewaters of main microlandscapes in each site are listed in **Table 2**. The mean values for the whole WSL territory for two dominant micro-landscapes, mound and hollow, are given in the last two columns of this table. Results of the application of Wilcoxon-Mann Whitney test for assessing the differences of DOC and several major and TE mean values between the dominant micro-landscapes in each site are listed in **Table S2** of **Supplement**. According to the chosen statistical criteria, only a few elements (DOC, Al, Fe, Si, Mn, Cu, Cd, Pb, Hf, U) depicted significant differences in their concentration between different micro-landscapes. The DOC was approximately twice higher ($p = 0.023$ to 0.043) in mounds (or polygons) compared to hollows in all 4 sites except Pangody, where the difference was only a factor of 1.1 which is not significant ($p = 0.082$). In Khanymey, Urengoy and Tazovsky, the order of DOC concentration in various micro-landscapes was (mound or polygon) ≥ (permafrost subsidence or frost crack) > hollow. Cu and, sometimes, Zn, followed this order. Concentrations of Al, Si, Fe, Sr did not demonstrate any systematic difference between positive and negative forms of relief for each site, without distinct preferential enrichment of one microlandscape versus another in the north or in the south. The minimal contrast in DOC and element concentration between micro-landscapes was observed in Pangody and the maximal variability was in Khanymey.

Within the standard deviation of the mean values, there was no difference in DIC, Si, Ca and Mg concentration between different micro-landscapes in all studied sites. The exception was Khanymey where the hollows demonstrated a factor of 1.5-2.8 higher Mg, Si and Ca concentration compared to mounds and Urengoy where the mounds contained less Mg and Si than the hollows. However, in the latter case, at $p = 0.041$ to 0.048, this difference was within the variation of the average (**Table S 2**). The mean concentrations of DIC, Cl, K, Si, Ca, Mg, Al, Fe, Ti, Sr, Ba, Zn, Mn, Ni and TE over the full WSL territory are quite similar (±20%) between positive and negative forms of relief (compare the last two

columns of Table 2). The DOC, B, Na, V, Ga, Cu, Cs, Pb, REE and Th exhibited a factor of 1.5±0.2 (significant at $p < 0.05$) higher WSL-mean concentrations in mounds/polygons compared to hollows.

### 3.3. Effect of latitude and permafrost zone on peat porewater concentrations of DOC and metals

In order to examine the latitudinal trend of element concentration in the porewater, first we run the Kruskal-Wallis and then the Wilcoxon-Mann Whitney pair test for overall differences. After that we assessed, which micro-landscape exhibited the largest difference between sites. Results include the p-value of the difference between one given site and other sites located northward (**Table S3** of the Supplement). The difference between sites was tested for mounds/polygons and hollows for all 5 sites and for permafrost subsidence/frost crack for 3 most northern sites (Khanymey, Urengoy and Tazovskiy). The DOC and major elements (Ca, K, Al, Si, Fe) exhibited clear difference ($p < 0.05$) between different geographic zones. The most pronounced difference between pair sites was observed for hollows. Thus, the porewaters from hollows in most southern site (Kogalym, of the sporadic permafrost) demonstrated statistically significant differences in DOC, Ca, K, Al, Si, Ni, Cu, Sr, Rb concentrations from hollows of Khanymey, Pangody, Urengoy, and Tazovskiy. Among the elements listed in Table 2, DOC, Ca, Fe and Sr were found to be most sensitive to the latitude of the sampling site regardless of the type of micro-landscape.

The general latitudinal trend in element concentration together with mean values in each micro-landscape as a function of latitude was examined for all major and TE. The latitudinal trend was approximated by a linear regression using all micro-landscapes and individually for hollows and mound/polygons:

$$[\text{Element}] = A + B \times \text{Latitude (°N)} \quad (1)$$

where $A$ and $B$ are the element-specific empirical coefficients. Parameters of equation for each element are listed in **Table 3**. For most major components including DOC there was no systematic trend of increasing or decreasing of average concentration across the 640 km latitudinal profile. There was a local maximum of DOC concentrations in porewaters of peat mounds sampled at the Khanymey-Urengoy sites. Overall, 3 patterns of concentration – latitude dependence could be distinguished shown in **Figs. 3-5** and **S4-S5**:

(1) Specific Conductivity, pH, DIC, DOC, K, Na, SO4, Si, B, Li, Fe, Ti, Cr, Ba, Mo, As, light REEs (La, Ce), W, and U did not exhibit any statistically significant trend ($R^2 < 0.5$) or this trend was within the uncertainties as illustrated in **Fig. 3 A-H** and **Fig. S4 E-K**;

(2) A clear trend of steady increasing concentration northward was observed for $SUVA_{280}$, Mg, Ca, Al, Cu, V, Mn, Ni, Sr, heavy REEs, Zr, Hf, Th ($0.45 < R^2 < 0.62$, $p < 0.05$). The overall increase from sporadic to continuous permafrost zone ranged from a factor of 2 to a factor of 5, illustrated in **Fig. 4 A-H** and **Fig. S5 A-F**.

(3) Cl, Sb, Pb, Cd, Zn, Rb, and Cs exhibited a decreasing trend northward shown in **Fig. 5 A-E** ($0.48 < R^2 < 0.84$).

For some elements, there was a lack of any trend between 62°N and 66.5°N, followed by an increase (significant at $p < 0.05$) between 66 and 67.5°N: Ca (**Fig. 4 C**), Mn (**Fig. S5 A**), Co (**Fig. S5** B), V (**Fig. 4 F**) and As (**Fig. S4 H**). The most pronounced trend of element concentration increase northward was observed in mounds/polygons for Al ($R^2 = 0.91$), Sr ($R^2 = 0.69$), Zr ($R^2 = 0.57$), Ce ($R^2 = 0.76$), Hf ($R^2 = 0.68$) and Th ($R^2 = 0.92$). For these elements, the trend in hollows/cracks was much less pronounced or even absent, with $R^2 < 0.5$ (**Table 3**). A decreasing trend of element concentration northward was also better pronounced in mounds/polygons for Na, Cl, Rb, Cs and Pb.

## 4. Discussion

### 4.1. Dissolved organic carbon transport in peat soils

The first unexpected result of this study was the lack of significant decrease of DOC concentration in peat porewaters northward, from sporadic to discontinuous and continuous permafrost zone (**Fig. 3 C**). The character of the DOM also remained highly constant across the latitudinal / permafrost gradient as the $SUVA_{280}$ ranged from 2.4 to 3.5 L $mg^{-1}$ $m^{-1}$ in all sites regardless of the microlandscape, with weak increase northward (**Fig. 4 A**). These values of $SUVA_{280}$ are consistent with those of the lakes (2 to 4 L $mg^{-1}$ $m^{-1}$, Manasypov et al., 2015) and rivers (2 to 3.5 L $mg^{-1}$ $m^{-1}$, Pokrovsky et al., 2015) of the region during summer period. The previously published values of $SUVA_{280}$ in WSL surface waters were similar across a large scale of lake size (from 50 to 500,000 m²) and latitudinal position of the river watershed (from 57°N to 66°N). This strongly suggests highly uniform feeding of Siberian inland waters by allochthonous DOM originated from peat leaching within the soil profile. The DOC transport to the river and lake presumably occurs via suprapermafrost flow over the frozen peat layers at the depth ranging between 20 and 80 cm depending on the season, the latitude and the micro-landscape context (see Fig. 2). Given the similarity of $SUVA_{280}$ values across significant geographical transect on positive forms of micro-relief (**Fig. 4 A, Table 3**), we hypothesize the similarity of the nature of water-soluble OM that constitutes the peat on mounds. At the same time, sizeable increase in the $SUVA_{280\,nm}$ northward may indicate a higher aromaticity of soil porewater DOM in the continuous permafrost zone relative to discontinuous and sporadic permafrost zone (Fig. 4 A). The change of SUVA from 2.4 to 3.4 in hollows demonstrates a significant shift in the composition of the DOM and may have a pronounced effect upon the biogeochemical processing of DOM upon export as it has been recently shown in Eastern Siberia (Frey et al., 2016). This contradicts the conclusion reached in recent studies of surface waters and soil leachates that the DOM leached from the permafrost soil layer has a consistently lower concentration of aromatic carbon (i.e. lower $SUVA_{254}$ values, Mann et al., 2012; Cory et al., 2013, 2014; Abbott et al., 2014; Ward and Cory, 2015), compared to DOM draining from the active, organic surface layer. However, the majority of previous studies dealt with non-peat permafrost environment. In the case of the WSL peatland, the contribution of UV-transparent microbial exometabolites and plant exudates including low molecular weight organic acids (i.e., Giesler et al., 2006) is certainly much higher in the southern forest-tundra and taiga zone compared to northern sites of the polygonal tundra. In the present study, statistically significant increase of $SUVA_{280}$ northward in hollows ($R^2 = 0.599$, see Table 3) may also indicate the lower rates of DOM processing in soils in the north, linked to either shorter residence time of soil fluids or weaker processes of photo- and bio-degradation in continuous permafrost zone compared to sporadic and discontinuous zone.

Generally higher DOC concentration in porewaters of mounds compared to that of hollows (Table 2) has two possible explanations. The soluble DOC retainment by clay horizon that underlays the peat in the WSL was hypothesized as the main regulator of the DOC level in rivers of large latitudinal transect of WSL, from permafrost-free to continuous permafrost zone (Pokrovsky et al., 2015). The gradient consisted in increasing the DOC concentration northward of 64°N (Pokrovsky et al., 2015) because the DOC-adsorbing clay horizon that underlays the peat may be frozen in the north (Kawahigashi et al., 2004). The latter authors suggested that the DOC in northern, permafrost-affected tributaries of the Yenisey River was less biodegradable (and thus better preserved during its transport from the soil to the river) than that in southern tributaries. If true, the lower DOC concentrations in hollows and subsidence relative to the mounds observed in the present study is due to DOC adsorption on unfrozen mineral layers (silt, clays) located below the peat horizon in depressions and hollows, which have much deeper position of the ALT than the mounds (see Table 1 and Fig. 2). At the same time, if soil pore waters are affected by the presence of minerals, then it should impact primarily the lithogenic elements (Ca, Mg, Sr, Si, Ti, Al, Zr…) whose concentration should be higher in negative forms of relief relative to that in the positive ones. This hypothesis is not supported by the concentration pattern of inorganic

316 constituents of porewaters as shown in the next section. Note also that, because the mounds thaw later than hollows, the
317 period of unfrozen exchange of constituents in the soil with porewater is shorter in mounds compared to hollows.
318 However, this does not go in line with the observed difference of higher DOC and metal concentration in porewater of
319 mounds relative to hollows.

320 The 2nd explanation of the elevated DOC concentration in mounds compared to hollows across the whole
321 permafrost gradient is related to the time of reaction between the peat and the pore fluids. From detailed hydrological
322 studies on frozen peatbog of western Siberia, the water residence time in peat mound is a factor of 14 higher than that in
323 hollows and depressions (Novikov et al., 2009). The latter have much higher hydrological connectivity to surrounding
324 streams and temporary water channels and as such offer shorter contact time and pathways of vertically infiltrating and
325 laterally migrating water. During the summer baseflow period, up to 70-80% of watershed covered by mounds in frozen
326 peatland of western Siberia may remain disconnected from the hydrological network (Batuev, 2012). The mounds and
327 polygons are therefore essentially controlled by water evaporation, leading to evaporative concentration of DOC and
328 other solutes within the soil profile. The available data on water infiltration parameters of hollows and permafrost
329 subsidences located in discontinuous permafrost zone of the WSL demonstrate an order of magnitude faster water
330 migration in various depressions (hollows, subsidences) compared to mounds (Novikov et al., 2009 and unpublished data
331 of the authors on NaCl tracer migration in frozen polygons and palsa peatbogs of the WSL). The density of the peat in
332 the mounds and polygons is a factor of 2 to 10 higher than that in the hollows and depressions (Ivanov and Novikov,
333 1976). Thus an analogy of ground surface and deep peat can be used for comparison between negative and positive forms
334 of microrelief, respectively. In the peatland-dominated zone of discontinuous permafrost, the total porosity was reported
335 to drop by about 10% between the ground surface and 35 cm depth; however, the active porosity decreased by as much
336 as 40% over the same distance (Quinton et al., 2000). The saturated hydraulic conductivity of peat decreases rapidly with
337 depth (Quinton et al., 2009). It thus can be hypothesized that, in the dense peat on mounds and polygons, the pores are
338 significantly smaller with less interconnection, which leads to more restricted flow and greater turtuosity (Rezanezhad et
339 al., 2009, 2010, 2016). All these factors should increase the water residence time in pores of peat in mounds relative to
340 hollows and allow for efficient enrichment of peat porewater by DOC in the former.

341 The DOC pore water concentration invariance across the latitudinal gradient of the WSL is consistent with the
342 lack of peat thickness and thermal regime effect on pore water chemistry. First, the peat thickness did not exert a direct
343 impact on the degree of porewater enrichment in DOC among various micro-landscapes: there was no dependence
344 between the DOC concentration in porewater and the total thickness of the peat ($R^2 < 0.01$, not shown). Second, the
345 thermal regime of soil porewater is responsible neither for the difference between mounds and hollows nor for latitudinal
346 dependence of DOC concentration. The effect of temperature on peat leaching in aqueous solution is not known, but by
347 analogy with surface-controlled dissolution reaction of minerals (i.e., Schott et al., 2009) it can be by a factor of 2 to 3 for
348 each 10°C rise. Such a large difference in 10°C between different adjacent micro-landscape seems highly unlikely. This
349 is confirmed by both our field measurements in Tazovsky (mean annual temperature of peat at 5 cm depth is equal to -
350 1.9°C in mound and +1.9°C in hollow), and the observations of other researchers in the WSL. In the Nadym region
351 (discontinuous permafrost zone), the mean annual temperature of mounds and hollows is 1.0 and 1.6°C, respectively
352 (Bobrik et al., 2015). At the latitude of Urengoy-Tazovsky and Khanymey, the average difference between mound and
353 hollow of summer-time temperature at 20 cm depth is 2.9 and 3.4°C, respectively (Novikov et al., 2009). A similar
354 difference of peat temperature between mounds and depressions at 20 cm depth (< 4°C) was reported for the Noyabrsk
355 region (discontinuous permafrost zone, Makhatkov and Ermolov, 2015). Globally, the temperature of soil porewater

across the latitudinal gradient does not exceed 10°C (Novikov et al., 2009) which is not sufficient to exert any pronounced control on DOC concentrations.

To summarize, we hypothesize that *i*) the DOC concentration should be controlled by the DOC residence time and travel pathway through the organic topsoil and *ii*) the enrichment in DOM of the interstitial soil solution occurs via lichens, moss, litter and peat leaching. Although the runoff is known to exert the primary control on stream DOC export from the boreal peatland catchments (Olefeldt et al., 2013; Leach et al., 2016), the existing hydrological modeling of subsurface transport of dissolved carbon in a discontinuous permafrost zone suggests that both concentration and load of DOC are water flow-independent (Jantze et al., 2013). As such, it is the time of reaction between the peat and downward infiltrating waters that essentially controls the degree of peat pore-water enrichments in DOC. This time is presumably similar across significant permafrost and climate gradients.

### 4.2. Factors controlling major and trace element concentration in peat soil porewaters

Organic and organo-Fe, Al colloids dominate the speciation of most cations (including alkaline-earth metals) and TE in low-TDS humic surface waters of permafrost-affected WSL territory (Pokrovsky et al., 2016b), similar to other boreal catchments (Köhler et al., 2014). As a result, the behaviour of many major and TE in peat porewater is likely to follow that of DOC, Fe and Al as main colloidal carriers. The importance of colloidal Fe and Al as primary carriers of TE in peat soils is confirmed by results of this study: in pore-waters, none of the TE correlated with DOC ($R < 0.5$) whereas Fe and Al concentrations correlated with many TE such as Ti, V, Cr, Co, Ni, As, Sr, Zr, Nb, heavy REE, Hf. This is consistent with decoupling of $TE^{3+}$ and DOC during size separation procedure as two independent colloidal pools (high molecular weight Fe, Al-rich and low molecular weight $C_{org}$-rich), already demonstrated for European boreal rivers (Neubauer et al., 2013; Vasyukova et al., 2010) and other Siberian rivers and WSL thermokarst lakes (Pokrovsky et al., 2006; Pokrovsky et al., 2011, 2016b). At the same time, although organo-ferric and organo-aluminium colloids are certainly important factors of insoluble element transport in peat soil, the source of TE may become more limiting for overall concentration of TE in soil porewater than their speciation. There are two possible sources of "lithophile" elements in the peat and peat porewaters: atmospheric dust deposition at the moss and lichen surface and upward migration of soil fluids that carry mineral particles from underlying loam horizons. The loam horizons are rich in silicate clay minerals (e.g., Ovchinnikov et al., 1973; Golovleva et al., 2017) that contain insoluble elements. The geochemical analysis of TE distribution in WSL peat cores across the studied permafrost gradient allowed to distinguish several categories of TE depending on their source such as soluble atmospheric aerosols, atmospheric dust, underlying mineral layers, plant biomass, and surface water flooding (Stepanova et al., 2015). The atmospheric deposition of lithogenic elements in the form of soluble aerosols on the moss surfaces followed by incorporation into the peat is expected to be low as shown by thorough snow analyses across the large WSL gradient (Shevchenko et al., 2016). Therefore, atmospheric dust seems to be the main source of insoluble metals in WSL peat as it is also known from other northern bogs (Shotyk et al., 2016). Regardless of the origin of lithophile elements, we hypothesize that the leaching of insoluble trivalent and tetravalent hydrolysates ($TE^{3+}$, $TE^{4+}$) from solid phase to interstitial soil solution may be restricted by the availability of silicate clay minerals within the peat core.

Based on results of the PCA treatment (**Fig. S3 A, B**), the dendrogram of a hierarchical cluster **(Fig. S3 C**) and the correlations between elements (**Table S1**) we hypothesize that the source of Cr, V, Al, REEs, Nb, Zr, Hf, Th, U but also of Mg and Li is silicate minerals dispersed within the peat matrix. These elements exhibit the highest correlation with Si in porewaters and appear to be linked to the first factor (F1) of the PCA. The silicate minerals may originate from

both atmospheric dust and underlying clay/silt horizons. The lack of correlation of K, Rb, Mn, Ba, Mo, W, Zn, Pb, Cd, Cs, Sb with DOC, Fe or Al in peat porewaters of WSL (**Table S1**) can be explained by specificity of these elements. In particular, K, Rb, Mn, Cu, Ba are biotically-controlled by moss growth and thus unlikely to be linked to any mineral source (Stepanova et al., 2015). It seems also plausible that indifferent oxyanions (Mo, Sb, W) or disperse pollutants delivered by atmospheric deposition on moss surface followed by incorporation into peat (Zn, Cd, Pb, Sb, Tl) do not exhibit significant correlation with main colloidal components.

One can expect that dissolved element decreases its concentration in the peat porewater northward regardless of the micro-landscape due to *i*) decrease of the thickness of peat deposits in total and the active soil (peat) layer in particular (Beilman et al., 2009; Novikov et al., 2009: Stepanova et al., 2015) which decreases the amount of peat interacting with downward penetrating fluids; *ii*) decrease of plant biomass (Frey and Smith, 2007), which diminishes the amount of plant litter that can release the elements (Pokrovsky et al., 2006; Fraysse et al., 2010), and also decrease the plant ability to weather minerals within the soil profile (Moulton et al., 2000); *iii*) shortening the unfrozen period of the year leading to the decrease of the residence time of water in soil pores and *iv*) overall decrease of the intensity of chemical weathering, $CO_2$ consumption and riverine fluxes with mean annual temperature decrease (Dessert et al., 2003). However, an unexpected result of this study was that the overwhelming number of major and TE did not exhibit any statistically significant decreasing trend of concentration with latitude. Instead, we observed a measurable northward increase in concentration of a number of lithogenic elements, whose presence is known to mark the intensity of mineral weathering. These are Mg, Al, Ti, V, Sr, REEs, Zr, Hf and Th, originated from silicate minerals of the soil profile. For example, Al, Ba, Fe, and Mn were reported to reflect the mineral weathering as they exhibited elevated concentrations in Alaskan rivers during the late Fall, that correlated with the maximal depth of the thawed active layer (Barker et al., 2014). The mechanism related to enhanced mobilization of low-soluble elements during deepening of the ALT is penetration of DOM-rich surface fluids to deeper soil horizon and leaching of lithogenic elements from underlying mineral substances, in the form of strong organic complexes (chelates). This mechanism can be tested via comparison of lithogenic element concentration in contrasting micro-landscapes. Thus, Sr, which is considered as an indicator of mineral sources in surface waters of the permafrost zone (Keller et al., 2010; Bagard et al., 2011), was highly similar between mound and hollow or even higher in mounds than in hollows or subsidences (Table 2). Given that the negative forms of relief in the WSL exhibit higher proximity of thawed layer to the mineral horizon because of lower thickness of peat and deeper ALT (Tyrtikov, 1973; Lupachev et al., 2016), the lack of link between Sr concentration and ALT position within the peat-silt/clay profile suggests that the underlying minerals do not participate in feeding the soil solutions by lithogenic elements. Rather, aeolian (long-range) dust deposits throughout the territory may lead to incorporation of solid atmospheric particles into the moss biomass. Subsequently, it is the dissolution of agglutinated minerals that enriches the peat porewater in lithogenic elements, including Si. Moreover, the concentration of elements likely originated from silicate matrix (Al, Si, Fe) in hollows and subsidences did not exceed that in mounds. Taken into account that the position of the permafrost boundary is much closer to the mineral substrate in negative forms of relief compared to mounds (see Table 1 and Fig. 2), this strongly suggests the lack of element leaching from the underlain mineral matrix. As such, the observed trends of element concentration with latitude reflect the leaching of essentially peat constituents with associated silicate particles without interferences with massive deposits of underlying sand, clay and silt in various micro-landscapes. Following the same reasoning, the lack of DIC, Mg and Ca variation among the micro landscapes suggests a negligible role of silicate and carbonate mineral weathering within the peat profile.

In addition to evaporative concentration mechanism and the greater residence time of solutes in mound compared to hollows, identified for DOC pattern in section 4.1, the peat chemical composition may be different between negative and positive forms of relief and thus it can contribute to porewater enrichment in major and TE. Indeed, the degree of peat decomposition and elementary content of peat on mounds is higher than that on hollows and depressions (Stepanova et al., 2015): a comparison of peat elementary composition at 15 cm depth on Pangody site demonstrated a factor of 1.5 to 3.5 higher concentration in mounds compared to hollows of major (Ca, K, Na, Fe) and ~40 TE except Mg, Zn, Sb and Pb (a factor of 1.3 to 3 richer in hollows than in mounds).

The lack of increase of Cl, $SO_4$ and Na in peat porewaters from the most northern site (Tazovskiy) compared to the intermediate sites (Urengoy, Pandogy) dismisses the possibility of element leaching from frozen saline sediments abundant in the Russian Arctic Coast (e.g., Brouchkov, 2002). Presumably, these saline sediments are not in contact with soil and suprapermafrost waters even at the time of maximal ALT, as also inferred from riverwater geochemistry in the permafrost-affected region of WSL (Pokrovsky et al., 2015). The elements originated from marine aerosols such as Na, Cl, $SO_4$, B, Li, Rb, Cs exhibited a decreasing or indifferent, but not increasing trend of concentration northward. This precludes a strong influence of marine atmospheric deposition on surface water chemistry, unlike it was suggested in earlier works in this region (Syso, 2007; Smolyakov, 2000).

*4.3. Comparison of peat porewaters with rivers and thermokarst lakes*

The peat soil porewaters sampled above the position of the permafrost table can serve as representative sources of water and solutes prior to export to the thermokarst lakes and rivers (Fig. 2). Therefore, a first-order comparison of concentrations between these aquatic systems allows evaluation of the role of peat (shallow surface) versus mineral (deep subsurface and underground waters) feeding of Siberian inland waters. This comparison was based on mean values of DOC and TE concentration in porewaters for the whole permafrost-affected WSL territory (Table 2) and those previously published for lakes and rivers of the same latitudinal gradient (Manasypov et al., 2014 and Pokrovsky et al., 2015, 2016a). The dissolved components measured in rivers and lakes during summer period can be classified into three categories: (1) Rivers or lakes exceed soil porewaters by a factor of 3 to 10; (2) River or lakes are similar to porewaters within a factor of 2, and (3) Rivers or lakes are significantly lower (more than a factor of 3) than the porewaters. The elements of the first category are DIC, Ca, Mg, Si, B, Al, Mn, Na for rivers and only Si for lakes. The second category comprises DOC, Li, K, Rb, Fe, Ni, Co, Cr, As, Sr and U for rivers and Li, B, Na, K, Rb, Cs, Ca, Mg, Ti, V, Mn, Ni, Cu, Zn, Co, Cd, Sr, Mo, As, Sb for lakes. The 3$^{rd}$ category includes Ti, Cu, Pb, Cd, Mo and REEs for rivers and DOC, Al, Fe, Ga, Y, Zr, Ba, W, REEs, Th, U for lakes. This first-order comparison demonstrates that the soil porewaters alone are sufficient to provide the concentrations of all major and TE in lakes. In other words, the transport of soil porewaters along the permafrost boundary in the form of suprapermafrost flow may be the sole source of incoming solutes to thermokarst lakes of western Siberia, across all 3 permafrost zones. This hypothesis is fully consistent with the lack of any underground feeding of WSL thermokarst lakes, demonstrated in earlier studies (Manasypov et al., 2015).

In contrast to lakes that can be fully supplied by solutes from surrounding peat porewaters, the rivers require some “mineral” influx in addition to surface and shallow subsurface “organic” influx, in order to explain the elevated concentrations of DIC, Ca, Mg, Na, Si, Al in the riverwater relative to the peat porewater. This influx, mostly pronounced during summer baseflow period, may include the groundwater seeping via taliks on the river bed and shallow

subsurface flow over clays and silt deposits. This process is fairly well known for other, non-peatland permafrost setting (MacLean et al., 1999; Bagard et al., 2011; Barker et al., 2014; Tank et al., 2016).

The latitudinal dependences of element concentration in the peat pore water revealed in this study can be compared to the latitudinal dependences of DOC and element concentration in adjacent thermokarst lakes and rivers. The elementary trends in the inland waters of western Siberia were associated to the influence of marine aerosols or long-range atmospheric transport of industrial pollutants in lakes (Manasypov et al., 2014) and the evolution of chemical composition of the peat and underlying mineral deposits in rivers (Pokrovsky et al., 2015; 2016a). However, the possible links are not straightforward and valid only for a small number of elements. Thus, increasing concentrations of Ca, Ni and Sr (**Fig. 4C, 4G, 4H**, respectively) and decreasing concentration of Sb and Pb (**Fig. 5 D and E,** respectively) northward are consistent with the trend in thermokarst lakes of western Siberia from 63°N to 71°N (Manasypov et al., 2014). However, the other elements exhibiting a clear increasing (K, Cu, Mo) or decreasing (V, Ba) latitudinal trend in lakes (Manasypov et al., 2014) do not show such a trend in peat pore-waters sampled in this study. Presumably, variable and simultaneously acting processes control the delivery of element from the peat core to the adjacent lakes over the permafrost gradient.

Because the leaching of peat constituents by downward penetrating fluids is very fast and weakly depends on temperature and local hydrological pathway within the peat pores, one can expect that the global hydrological setting will primarily control the peat weathering intensity. As such, it is the amount of water that passes through the peat soil column before being evacuated to the river that defines the overall export fluxes of elements from the peatland to the hydrological network. This prediction is consistent with reported higher riverine fluxes of DOC, Si and cations in the northern region of the WSL (66.5 to 67.5°N) relative to the southern region (62-65°N) of this territory corresponding to higher surface runoff in the north (Pokrovsky et al., 2015).

The fluxes of Ca, Mg and $HCO_3^-$ ions carried by rivers are used for calculation the $CO_2$ uptake flux due to chemical weathering, i.e., reaction of atmospheric $CO_2$ with Ca, Mg-bearing silicate minerals (Dessert et al., 2003; Beaulieu et al., 2012). Not more than 10% of total riverine flux of Ca, Mg and $HCO_3$ is considered to be due to atmospheric input. An important consequence of our obtained results on soil porewaters in the WSL is that the intensity of chemical weathering and associated $CO_2$ consumption in the permafrost regions (i.e., Beaulieu et al., 2012) by small rivers without pronounced underground feeding in peatlands could be overestimated relative to the regions with shallow organic soil horizons. As a result, the flux of DIC and major cations in the peatland-draining rivers should be corrected for the input of these elements via peat pore-water discharge to the river main stream. For a number of small rivers ($S_{watershed}$ < 1000 km²) in the permafrost zone of the WSL that are fed by shallow surface runoff through the peat horizon, this correction can range from 20 to 80% of total riverine DIC, Ca and Mg flux. The global consequence of this correction is that the continental-weathering $CO_2$ sink in northern peatland regions might be a factor of 2 to 4 smaller than that currently deduced from the fluxes of large rivers.

*4.4. Prospective for climate change in western Siberia*

In accordance with a common scenario of the climate change in the subarctic, a shift of the permafrost boundary further north and the increase of the active layer thickness are anticipated in the WSL (Pavlov and Moskalenko, 2002; Frey and McClelland, 2009; Moskalenko, 2009; Romanovsky et al., 2010; Vasiliev et al., 2011; Anisimov et al., 2013). This agrees with large-scale permafrost shifts consisting in southern boundaries moving northward (see Walvoord and

Kurylyk, 2016 for a review). Assuming a "substitution space for time" scenario, and upscaling the data of peat pore waters obtained in this study, we predict that the shift of the permafrost boundary northward even by 2° latitude will not affect the concentrations of most major and TE in peat pore-waters. The concentrations of DOC, DIC, Ca, Mg, K, Al, Fe, and trace metals in continuous permafrost zone may remain constant or decrease by a factor of 1.5 to 2 which is often within the natural variation between different microlandscapes, soil depths and seasons.

The ALT is projected to deepen more than 30% during this century in the Northern Hemisphere (Anisimov et al., 2002; Stendel and Christensen, 2002; Dankers et al., 2011). As a general scenario in frozen peatlands of the subarctic, this increase will bring about the involvement of mineral horizons into water infiltration zone downward the soil profile (Walvoord and Kurylyk, 2016). The degradation of peat mounds and polygons will be accompanied by the spreading of hollows and depressions (Pastukhov and Kaverin, 2016). As a result, the water coverage of the watershed will increase thus enhancing the anaerobic conditions. On the one hand, this will increase the fraction of hollows and depressions containing less concentrated interstitial soil solutions and thus the stock of DOC, major elements and trace metals in soil fluids will decrease. On the other hand, the increasing anaerobic conditions may preferentially mobilize redox sensitive elements (Fe, Mn, Cr, V…) from the peat to the porewaters. Overall, the share of spring runoff from the mounds to the rivers and lakes will decrease whereas during the summer baseflow, the input from the hollows and depressions to the hydrological network will increase.

The concept "substituting space for time" allows foreseeing the consequences of soil warming in the continuous permafrost zone of the WSL peatlands on the adjacent river chemistry and export of carbon and metals from the watersheds. This prediction can be made only for small rivers of the WSL (e.g., watershed area < 10,000 km²) which drain the adjacent peatlands, have no underground feeding and flow essentially during unfrozen period of the year (see Pokrovsky et al., 2015, 2016a). For this, two basic scenarios can be considered: (*i*) a constant latitudinal pattern of permafrost distribution (no boundary migration) but complete disappearance of peat mounds and their replacement by hollows and depressions and (*ii*) a shift of the permafrost boundary to the north and transformation of the continuous permafrost zone into the discontinuous and transformation of the discontinuous permafrost into the sporadic without changing the microlandscape distribution. As a first approximation, we assume no change in precipitation, evapotranspiration and riverine runoff in the northern part of WSL (60-68°N), given that the drying trend will be pronounced only in the regions located to the south of 60 °N (Alexandrov et al., 2016).

The first scenario yields a decrease in the concentrations of DOC, DIC, major cations and trace metals in porewaters of continuous permafrost zone by not more than 30%. This estimation stems from the maximal difference in element concentration between mounds and hollows (Table 2) and typical proportion of mounds in the terrestrial landscape of the WSL (35±15 %, Novikov et al., 2009 and authors' unpublished data). The second scenario is based on the latitudinal patterns of element concentration in the peat porewaters (Table 3 and Figs 3-5, S4, S5). For this, a linear dependence of element concentration in all microlandscapes on the latitude given in Figs. 3 to 5 can be used. A two-degree northward shift in the position of the permafrost boundaries will bring about a factor of 1.3±0.2 decrease in Ca, Mg, Sr, Al, Fe, Ti, Mn, Ni, Co, V, Zr, Hf, Th, and REEs concentration in continuous and discontinuous permafrost zones. Note that a possible decrease in DOC, $SUVA_{280}$, Ca, Mg, Fe, Sr will not exceed 20% of their actual values. Finally, there may be an increase in Cl, Na, K, Rb, Cs, Zn, P and Sb concentration by 30±10%. In both scenarios of permafrost thawing in the WSL peatlands we do not expect any sizeable increase of soil porewater concentration in DOC and metal and enhancement of the export of solutes by small-size rivers which are not connected to the underground reservoirs. This contradicts the dominating paradigm of the increase of DOC, DIC, major cations and metal discharge

from the land to the ocean upon the on-going climate warming in other permafrost regions. Combining both scenario of permafrost thaw (northward permafrost boundary shift and extending the hollows over mounds) suggests that over the first decades, relatively fast permafrost coverage shift will not be accompanied by the change of micro-landscapes and thus the overall decrease of DOC and metal concentration in peat porewaters will be around 20 to 30%. The average rate of peat formation in Siberian flat-mound bogs is 0.24 mm $y^{-1}$ (Inisheva et al., 2013). Thus, taking into account the climate warming and accelerated peat growth, after 500 to 1000 years which are necessary to form the new ca. 20-cm peat layer, the second scenario will take over and thus up to 2-fold cumulative element concentration decrease in soil fluids of continuous permafrost zone may occur. Assuming a dominant feeding of small rivers by soil porewaters transported along the permafrost boundary, a slight decrease (i.e., < 30 %) of riverine transport of DOC, DIC, Fe, Al, Ca, Mg from the northern part of the WSL territory to the Arctic Ocean is anticipated. This decrease will be mostly pronounced for small rivers such as those of the Arctic coastal zone.

## Conclusions

A snopshot of peat soil water chemistry allowed to quantify the distribution of DOC, major and trace element in peat porewaters at the end of the active period across a sizeable gradient of permafrost. We did not confirm a trend of diminishing DOC and metal concentration in peat porewaters northward, despite a decrease in mean annual temperature, vegetation density and the active layer thickness. DOC, DIC and most major and TE did not exhibit any statistically significant trend of concentration with the latitude. A clear trend of increasing concentrations of Mg, Ca, Al, Ti, V, Ni, Sr, heavy REE, Zr, Hf and Th marked the increase of the influence of silicate mineral weathering. Concentrations of DOC, $SO_4^{2-}$, B, V, Cs, Th in pore waters in the peat mounds usually exceeded those in hollows and permafrost subsidences. The water residence time in peat of various densities and the peat chemical composition werehypothesized to be the main factors controlling the degree of element leaching from the peat column to the pore fluids. Applying a "substituting space for time" approach for the climate warming scenario in the WSL, we predict that the northward migration of permafrost boundary and the replacement of thawing frozen peat mounds and polygons by hollows, depressions and subsidences will decrease the concentrations of DOC, DIC, major cations and trace metals in porewater of continuous permafrost zone by a factor of 1.3±0.2. This in turn will decrease the feeding of small rivers and lakes by peat soil leachates and the overall export of DOC and metals from the WSL territory to the Arctic Ocean may decrease. As such, the dominating paradigm of the increase of DOC, DIC, major cation and metal export fluxes upon the on-going climate warming in boreal and subarctic regions should be revised for the case of frozen peatlands.

## Data availability

Full data set of major and trace element concentration in porewaters (< 0.45 μm) across the latitudinal profile of Western Siberia Lowland is available at the Research Gate, https://www.researchgate.net/publication/313058330_Element_concentrations_in_peat_soil_solutions_across_the_micro-landscapes_and_permafrost_zones_of_western_Siberia_peatlands

## Acknowledgements

We acknowledge support from RFBR Nos. 16-34-60203 mol_a_dk, BIO-GEO-CLIM grant from the Russian Ministry of Science and Education and Tomsk State University (No 14.B25.31.0001), RFFI grants No 15-29-02599, 17-55-16008,

FCP “Kolmogorov” Minobrnauki RF RFMEFI58717X0036, and a partial support from and RSF (RNF) grant No 15-17-10009 “Evolution of thermokarst ecosystems”.

## References


Abbott, B. W., Larouche, J. R., Jones Jr., J. B., Bowden, W. B., and Balser, A. W.: Elevated dissolved organic carbon biodegradability from thawing and collapsing permafrost, J. Geophys. Res.-Biogeo., 119, 2049–2063, 2014.

Akerman, H. J., Johansson, M.: Thawing permafrost and thicker active layers in sub-arctic Sweden, Permafrost Periglacial Process., 19, 279–292, 2008.

Alexandrov, G. A., Brovkin, V. A., and Kleinen, T. : The influence of climate on peatland extent in Western Siberia since the Last Glacial Maximum, Sci. Reports, 6, 24784, doi:10.1038/srep24784, 2016.

Anisimov, O. A., Shiklomanov, N. I. and Nelson, F. E.: Variability of seasonal thaw depth in permafrost regions: A stochastic modeling approach, Ecol. Model., 153, 217–227, 2002.

Anisimov, O., Kokorev, V. and Zhil'tsova, Y.: Temporal and spatial patterns of modern climatic warming: Case study of Northern Eurasia, Climat. Change, 118, 871–883, 2013.

Beaulieu, E., Godderis, Y., Donnadieu, Y., Labat, D., and Roelandt, C.: High sensitivity of the continental-weathering carbon dioxide sink to future climate change, Nat. Clim. Change, 2, 346–349, 2012.

Bagard, M. L., Chabaux, F., Pokrovsky, O. S., Prokushkin, A. S., Viers, J., Dupré, B., and Stille, P.: Seasonal variability of element fluxes in two Central Siberian rivers draining high latitude permafrost dominated areas, Geochim. Cosmochim. Ac., 75, 3335–3357, 2011.

Bagard, M. L., Schmitt, A. D., Chabaux, F., Pokrovsky, O. S., Viers, J., Stille, P., Labolle, F., and Prokushkin, A. S.: Biogeochemistry of stable Ca and radiogenic Sr isotopes in larch-covered permafrost-dominated watersheds of Central Siberia, Geochim. Cosmochim. Ac., 114, 169–187, 2013.

Batuev, V. I.: Formation of water runoff from mound bogs (case study of Western Siberia), TSPU Bulletin, 122(7), 146–152, 2012.

Barker, A. J., Douglas, T. A., Jacobson, A. D., McClelland, J. W., Ilgen, A. G., Khosh, M. S., Lehn, G. O., and Trainor, T. P.: Late season mobilization of trace metals in two small Alaskan arctic watersheds as a proxy for landscape scale permafrost active layer dynamics, Chem. Geol., 381, 180–193, 2014.

Beilman, D. W., MacDonald, G. M., Smith, L. C., and Reimer, P. J.: Carbon accumulation in peatlands of West Siberia over the last 2000 years, Global Biogeochem. Cy., 23(1), GB1012, doi:10.1029/2007GB003112, 2009.

Botch, M. S., Kobak, K. I., Vinson, T. S., and Kolchugina, T. P.: Carbon pools and accumulation in peatlands of the former Soviet Union, Global Biogeochem. Cy., 9(1), 37–46, doi:10.1029/94GB03156, 1995.

Blodau, C. and Moore, T. R.: Experimental response of peatland carbon dynamics to a water table fluctuation, Aquat. Sci., 65–47, doi:10.1007/s000270300004, 2003.

Bobrik, A. A., Goncharova, O. Yu., Matyshak, G. V., Ryzhova, I. M., Moskalenko, N. G., Ponomareva, O. E., Ogneva, O. A.: Relationship of active layer thickness and landscape parameters of peatlands in the north of west Siberia (Nadym station), Earth's Cryosphere, XIX(4), 31–38, 2015.

Brouchkov, A.: Nature and distribution of frozen saline sediments on the Russian Arctic Coast, Permafrost Periglacial Proc., 13, 83–90, 2002.

Brown, J., Ferrians Jr, O. J., Heginbottom, J. A., and Melnikov, E. S.: Circum-arctic map of permafrost and ground ice conditions, Boulder, CO 80309-0449 USA, National Snow and Ice Data Center, Digital media, 1998, revised February 2001.

Charman, D. J., Beilman, D. W., Blaauw, M., Booth, R. K., Brewer, S., Chambers, F. M., Christen, J. A., Gallego-Sala, A., Harrison, S. P., Hughes, P. D. M., Jackson, S. T., Korhola, A., Mauquoy, D., Mitchell, F. J. G., Prentice, I. C., van der Linden, M., De Vleeschouwer, F., Yu, Z. C., Alm, J., Bauer, I. E., Corish, Y. M. C., Garneau, M., Hohl, V., Huang, Y., Karofeld, E., Le Roux, G., Loisel, J., Moschen, R., Nichols, J. E., Nieminen, T. M., MacDonald, G. M., Phadtare, N. R., Rausch, N., Sillasoo, Ü., Swindles, G. T., Tuittila, E.-S., Ukonmaanaho, L., Väliranta, M., van Bellen, S., van Geel, B., Vitt, D. H., and Zhao, Y.: Climate-related changes in peatland carbon accumulation during the last millennium, Biogeosciences, 10, 929-944, doi:10.5194/bg-10-929-2013, 2013.

Clark, J. M., Heinemeyer, A., Martin, P., and Bottrell, S. H.,: Processes controlling DOC in pore water during simulated drought cycles in six different UK peats, Biogeochemistry, 109(1–3), 109–253, doi:10.1007/s10533-011-9624-9, 2012.

Cory, R. M., Crump, B. C., Dobkowski, J. A., and Kling, G. W.: Surface exposure to sunlight stimulates CO2 release from permafrost soil carbon in the Arctic, Proc. Natl. Acad. Sci. USA, 110, 3429–3434, 2013.

Dankers, R., Burke, E. J., Price, J.: Simulation of permafrost and seasonal thaw depth in the JULES land surface scheme, Cryosphere, 5(3), 773–790, 2011.

Dielemann, C. M, Lindo, Z., McLaughlin, J. W., Craig, A. E., Branfireum, B. A.: Climate change effects on peatland decomposition and porewater dissolved organic carbon biogeochemistry, Biogeochemistry, 128, 385–396, 2016.

Dessert C., Dupré B., Gaillardet J., Francois L., Allegre C.J.: Basalt weathering laws and the impact of basalt weathering on the global carbon cycle. Chem. Geol., 202, 257–273, 2003.
Drake, T. W., Wickland, K. P., Spencer, R. G. M., McKnight, D. M., Striegl, R. G.: Ancient low–molecular-weight organic acids in permafrost fuel rapid carbon dioxide production upon thaw, PNAS, 112(45), 13946–13951, doi:10.1073/pnas.1511705112, 2015.
Feng, X. J., Vonk, J. E., van Dongen, B. E., Gustafsson, O., Semiletov, I. P., Dudarev, O. V., Wang, Z. H., Montlucon, D. B., Wacker, L., and Eglinton, T.I.: Differential mobilization of terrestrial carbon pools in Eurasian Arctic river basins, P. Natl. Acad. Sci. USA, 110, 14168–14173, 2013.
Fouché, J., Keller, C., Allard, M., Ambrosi, J. P.: Increased $CO_2$ fluxes under warming tests and soil solution chemistry in Histic and Turbic Cryosols, Salluit, Nunavik, Canada, Soil Biol. Biochem., 68, 185–199, doi:10.1016/j.soilbio.2013.10.007, 2014.
Fraysse, F., Pokrovsky, O.S., Meunier, J-D.: Experimental study of terrestrial plant litter interaction with aqueous solutions, Geochim. Cosmochim. Acta, 74, 70–84, 2010.
Frey, K. E. and Smith, L. C.: Amplified carbon release from vast West Siberian peatlands by 2100, Geophys. Res. Lett., 32, L09401, doi:10.1029/2004GL022025, 2005.
Frey, K. E., McClelland, J. W., Holmes, R. M., and Smith, L. C.: Impacts of climate warming and permafrost thaw on the riverine transport of nitrogen and phosphorus to the Kara Sea, J. Geophys. Res., 112, G04S58, doi:10.1029/2006JG000369, 2007a.
Frey, K. E., Siegel, D. I. and Smith, L. C.: Geochemistry of west Siberian streams and their potential response to permafrost degradation, Water Resources Res., 43, W03406, doi:10.1029/2006WR004902, 2007b.
Frey, K. E. and Smith, L. C.: How well do we know northern land cover? Comparison of four global vegetation and wetland products with a new ground-truth database for West Siberia, Global Biogeochem. Cy., 21, GB1016, doi:10.1029/2006GB002706, 2007.
Frey, K. E. and McClelland, J. W.: Impacts of permafrost degradation on arctic river biogeochemistry, Hydrol. Process., 23, 169–182, 2009.
Frey, K. E., Sobczak, W. V., Mann, P. J., and Holmes, R. M.: Optical properties and bioavailability of dissolved organic matter along a flow-path continuum from soil pore waters to the Kolyma River mainstem, East Siberia, Biogeosciences, 13, 2279-2290, doi:10.5194/bg-13-2279-2016, 2016.
Gangloff, S., Stille, P., Schmitt, A.-D., Chabaux, F.: Factors controlling the chemical composition of colloidal and dissolved fractions in soil solutions and the mobility of trace elements in soils, Geochim. Cosmochim. Acta, 189, 37–57. doi:10.1016/j.gca.2016.06.009, 2016.
Geibe, C.E., Danielsson, R., van Hees, P.A.W., Lundström, U.S.: Comparison of soil solution chemistry sampled by centrifugation, two types of suction lysimeters and zero-tension lysimeters, Appl. Geochem., 21(12), 2096-2111, doi: 10.1016/j.apgeochem.2006.07.010, 2006.
Gentsch, N., Mikutta, R., Alves, R. J. E., Barta, J., Capek, P., Gitte, A., Hugelius, G., Kuhry, P., Lashchinskiy, N., Palmtag, J., Richter, A., Santrucková, H., Schnecker, J., Shibistova, O., Urich, T., Wild, B., and Guggenberger, G.: Storage and transformation of organic matter fractions in cryoturbated permafrost soils across the Siberian Arctic, Biogeosciences, 12, 4525–4542. doi:10.5194/bg-12-4525-2015, 2015.
Giesler, R., Högberg, M. N., Strobel, B. W., Richter, A., Nordgren, A., and Högberg, P.: Production of dissolved organic carbon and low-molecular weight organic acids in soil solution driven by recent tree photosynthate, Biogeochemistry, 84, 1–12, 2006.
Giesler, R., Lyon, S. W., Mörth, C.-M., Karlsson, J., Karlsson, E. M., Jantze, E. J., Destouni, G., and Humborg, C.: Catchment-scale dissolved carbon concentrations and export estimates across six subarctic streams in northern Sweden, Biogeosciences, 11, 525–537, doi:10.5194/bg-11-525-2014, 2014.
Goldberg, S. D., Knorr, K.-H., Blodau, C., Lischeid, G., Gebauer G.: Impact of altering the water table height of an acidic fen on $N_2O$ and NO fluxes and soil concentrations, Global Change Biol., 16(1), 220, doi:10.1111/j.1365-2486.2009.02015.x, 2010.
Golovleva, Yu. A., Avetov, N. A., Bruand, A., Kiryushin, A. V., Tolpeshta, I. I., Krasil'nikov, P. V.: Genesis of taiga poorly differentiated soils in West Siberia, Lesovedenie, № 2, 83–93, 2017, http://lesovedenie.ru/index.php/forestry/article/view/983 (in Russian).
Griffiths, N., Sebestyen, S. D.: Dynamic vertical profiles of peat porewater chemistry in a northern peatland, Wetlands, 36(6), 1119-1130, 2016.
Grosse, G., Goetz, S. J., McGuire, A. D., Romanovsky, V. E., Schuur, E. A. G.: Changing permafrost in a warming world and feedbacks to the Earth system, Environ. Res. Lett., 11(4), 040201, 2016.
Guo, L., Ping, C. L., and MacDonald, R.W.: Mobilization pathways of organic carbon from permafrost to Arctic rivers in a changing climate, Geophys. Res. Lett., 34, L13603, doi:10.1029/2007GL030689, 2007.
Haapalehto, T., Vasander, H., Jauhiainen, S., Tahvanainen, T., Kotiaho, J. S.: The effects of peatland restoration on water table depth, elemental concentrations, and vegetation: 10 years of changes, Restor Ecol., 19, 587–598, 2011.
Hendershot, W. H., Savoie, S., Courchesne, F.: Simulation of stream-water chemistry with soil solution and groundwater flow contributions, J Hydrol., 136(1–4), 237–252, doi:10.1016/0022-1694(92)90013-L, 1992.

Holmes, R. M., McClelland, J. W., Peterson, B. J., Tank, S. E., Bulygina, E., Eglinton, T. I., Gordeev, V. V., Gurtovaya, T. Y., Raymond, P. A., Repeta, D. J., Staples, R., Striegl, R. G., Zhulidov, A. V., and Zimov, S. A.: Seasonal and annual fluxes of nutrients and organic matter from large rivers to the Arctic Ocean and surrounding seas, Estuar. Coast., 35, 369–382, doi:10.1007/s12237-011-9386-6, 2012.

Herndon, E. M., Yang, Z., Bargar, J., Janot, N., Regier, T. Z., Graham, D. E., Wullschleger, S. D., Gu, B., Liang, L.: Geochemical drivers of organic matter decomposition in arctic tundra soils, Biogeochemistry, 126(3), 397–414, doi:10.1007/s10533-015-0165-5, 2015.

Holmes, R. M., Coe, M. T., Fiske, G. J., Gurtovaya, T., McClelland, J. W., Shiklomanov, A. I., Spencer, R. G. M., Tank, S. E., Zhulidov, A. V.: Climate change impacts on the hydrology and biogeochemistry of Arctic Rivers, in: Climatic Changes and Global warming of Inland Waters: Impacts and Mitigation for Ecosystems and Societies, Goldman, C. R., Kumagi, M., and Robarts, R. D., John Wiley and Sons, Ltd., Publication, The Atrium, Southern Gate, Chichester, West Sussex, UK, 1–26, 2013.

Hodgkins, S. B., Tfaily, M. M., McCalley, C. K., Logan, T. A., Crill, P. M., Saleska, S. R., Rich, V. I., Chanton, J. P.: Changes in peat chemistry associated with permafrost thaw increase greenhouse gas production, PNAS, 111(16), 5819–5824, doi:10.1073/pnas.1314641111, 2014.

Hodgkins, S. B., et al.: Elemental composition and optical properties reveal changes in dissolved organic matter along a permafrost thaw chronosequence in a subarctic peatland, Geochim. Cosmochim. Acta, 187, 123–140, 2016.

Ilina, S. M., Drozdova, O. Y., Lapitskiy, S. A., Alekhin, Y. V., Demin, V. V., Zavgorodnyay, Y. A., Shirokova, L. S., Viers, J., Pokrovsky, O. S.: Size fractionation and optical properties of dissolved organic matter in the continuum soil solution-bog-river and terminal lake of a boreal watershed, Organic Geochem., 66, 14–24. doi:10.1016/j.orggeochem.2013.10.008, 2014.

Inisheva, L. I., Kobak, K. I., Turchinovich, I. E.: Evolution of the paludification process, and carbon accumulation rate in bog ecosystems of Russia, Geography Natural Resources, 34 (3), 246–253, doi:10.1134/S1875372813030086, 2013.

Ivanov, K. E., Novikov, S. M.: Bogs of western Siberia, their composition and hydrological regime, Leningrad, Gidrometeoizdat, 448 pp., 1976 (in Russian).

Jantze, E. J., Lyon, S. W., and Destouni, G.: Subsurface release and transport of dissolved carbon in a discontinuous permafrost region, Hydrol. Earth Syst. Sc., 17, 3827–3839, doi:10.5194/hess-17-3827-2013, 2013.

Jessen, S., Holmslykke, H. D., Rasmussen, K., Richardt, N., Holm, P. E.: Hydrology and pore water chemistry in a permafrost wetland, Ilulissat, Greenland, Water Resources Res., 50(6), 4760–4774, doi:10.1002/2013WR014376, 2014.

Jorgenson, M. T., Harden, J., Kanevskiy, M., O'Donnel, J., Wickland, K., Ewing, S., Manies, K., Zhuang, Q., Shur, Y., Striegl, R., Koch, J.: Reorganization of vegetation, hydrology and soil carbon after permafrost degradation across heterogeneous boreal landscapes, Environ. Res. Lett., 8, Art No 035017, doi: 10.1088/1748-9326/8/035017, 2013.

Kaiser, C., Meyer, H., Biasi, C., Rusalimova, O., Barsukov, P., and Richter, A.: Conservation of soil organic matter through cryoturbation in arctic soils in Siberia, J. Geophys. Res., 112, 9–17, 2007.

Karavanova, E. I., Malinina, M. S.: Spatial and temporal variation in the elemental composition of soil solution from gleyic peaty-podzolic soils, Eurasian Soil Sci., 40(8), 830–838, doi:10.1134/S1064229307080042, 2007.

Kawahigashi, M., Kaiser, K., Kalbitz, K., Rodionov, A., and Guggenberger, G.: Dissolved organic matter in small streams along a gradient from discontinuous to continuous permafrost, Glob. Change Biol., 10, 1576–1586, doi:10.1111/j.1365-2486.2004.00827.x, 2004.

Keller, K., Blum, J. D. and Kling, G. W.: Stream geochemistry as an indicator of increasing permafrost thaw depth in an Arctic watershed, Chem. Geol., 273, 76–81, 2010.

Koch, J. C., Runkel, R. L., Striegl, R., McKnight, D. M.: Hydrologic controls on the transport and cycling of carbon and nitrogen in a boreal catchment underlain by continuous permafrost, J. Geophys. Res. – Biogeosciences, 118(2), 698–712, doi:10.1002/jgrg.20058, 2013.

Köhler, S. J., Lidman, F. and Laudon, H.: Landscape types and pH control organic matter mediated mobilization of Al, Fe, U and La in boreal catchments, Geochim. Cosmochim. Acta, 135, 190–202, 2014.

Kokelj, S. V., Jenkins, R. E., Milburn, D., Burn, C. R., Snow, N.: The influence of thermokarst disturbance on the water quality of small upland lakes, Mackenzie Delta Region, Northwest Territories, Canada, Permafrost Periglacial Res., 16, 343–353, doi:10.1002/ppp.536, 2005.

Kokelj, S. V., Zajdlik, B., Thompson, M. S.: The impacts of thawing permafrost on the chemistry of lakes across the subarctic boreal-tundra transition, Mackenzie Delta region, Canada. Permafrost Periglacial Res., 20(2), 185–199, doi:10.1002/ppp.641, 2009.

Kremenetski, K. V., Velichko, A. A., Borisova, O. K., MacDonald, G. M., Smith, L. C., Frey, K. E., and Orlova, L. A.: Peatlands of the West Siberian Lowlands: Current knowledge on zonation, carbon content, and Late Quaternary history, Quaternary Sci. Rev., 22, 703–723, 2003.

Laurion, I., Vincent, W.F., MacIntyre, S., Retamal, L., Dupont, C., Francus, P., Pienitz, R.: Variability in greenhouse gas emissions from permafrost thaw ponds, Limnol. Oceanogr., 55, 115–133, 2010.

Leach, J. A., Larsson, A., Wallin, M. B., Nilsson, M. B., and Laudon, H.: Twelve year interannual and seasonal variability of stream carbon export from a boreal peatland catchment, J. Geophys. Res. Biogeosci., 121, 1851–1866, doi:10.1002/2016JG003357, 2016.

Liu, L., Chen, H., Zhu, Q., Yang, G., Zhu, E., Hu, J., Peng, C., Jiang, L., Zhan, W., Ma, T., He, Y., Zhu, D.: Responses of peat carbon at different depths to simulated warming and oxidizing, Sci. Total Environ., 548–549, 429–440. doi:10.1016/j.scitotenv.2015.11.149, 2016.

Lobbes, J. M., Fitznar, H. P., and Kattner, G.: Biogeochemical characteristics of dissolved and particulate organic matter in Russian rivers entering the Arctic Ocean, Geochim. Cosmochim. Ac., 64, 2973–2983, 2000.

Lupachev, A. V., Gubin, S. V., Veremeeva, A. A., Kaverin, D. A., Pastukhov, A. V., Yakimov, A. S.: Microrelief of the permafrost table: structure and ecological functions, Earth's Cryosphere, XX(2), 3–14, 2016.

MacLean, R., Oswood, M. W., Irons, J. G. III, McDowell, W. H.: The effect of permafrost on stream biogeochemistry: A case study of two streams in the Alaskan (USA) taiga, Biogeochemistry, 47, 239–267, 1999.

Makhatkov, I. D., Ermolov, Yu. V.: The thermal regime of active layer of pit-covered terrain in northern taiga, Mezhdunarodnyi Zhurnal Prikladnukh i Fundamentalnukh Issledovanii (Internat. J. Appl. Fund. Studies), 215(11), 400–407, 2015.

Manasypov, R. M., Pokrovsky, O. S., Kirpotin, S. N. and Shirokova, L. S.: Thermokarst lake waters across the permafrost zones of western Siberia, Cryosphere, 8, 1177–1193, 2014.

Manasypov, R. M., Vorobyev, S. N., Loiko, S. V., Kritzkov, I. V., Shirokova, L. S., Shevchenko, V. P., Kirpotin, S. N., Kulizhsky, S. P., Kolesnichenko, L. G., Zemtzov, V. A., Sinkinov, V. V. and Pokrovsky, O. S.: Seasonal dynamics of organic carbon and metals in thermokarst lakes from the discontinuous permafrost zone of western Siberia, Biogeosciences, 12, 3009–3028, 2015.

Manasypov, R. M., Shirokova, L. S. and Pokrovsky O. S.: Experimental modeling of thaw lake water evolution in discontinuous permafrost zone: role of peat and lichen leaching and ground fire, Sci. Tot. Environ., 580, 245-257, 2017.

Mann, P. J., Davydova, A., Zimov, N., Spencer, R. G. M., Davydov, S., Bulygina, E., Zimov, S., and Holmes, R. M.: Controls on the composition and lability of dissolved organic matter in Siberia's Kolyma River basin, J. Geophys. Res.-Biogeo., 117, G01028, doi:10.1029/2011JG001798, 2012.

Mann, P. J., Eglinton, T. I., Mcintyre, C. P., Zimov, N., Davydova, A., Vonk, J. E., Holmes, R. M., Spencer, R. G. M.: Utilization of ancient permafrost carbon in headwaters of Arctic fluvial networks, Nat Commun., 6, doi:10.1038/ncomms8856, 2015.

Marlin, C., Dever, L., Vachier, P., Courty, M. A.: Chemical and isotopic changes in soil-water during perfrosting of an active layer on continuous permafrost (Brogger-Peninsula, Svalbard), Canad. J. Earth Sci., 30(4), 806–813, 1993.

Mavromatis, V., Prokushkin, A. S., Pokrovsky, O. S., Viers, J., and Korets, M. A.: Magnesium isotopes in permafrost-dominated Central Siberian larch forest watersheds, Geochim. Cosmochim. Ac., 147, 76–89, 2014.

Michalzik, B., Kalbitz, K., Park, J.-H., Solinger, S. and Matzner, E.: Fluxes and concentrations of dissolved organic carbon and nitrogen - A synthesis for temperate forests, Biogeochemistry, 52, 173–205, 2001.

Morison, M.Q., Macrae, M. L., Petrone, R. M., Fishback, L.: Seasonal dynamics in shallow freshwater pond-peatland hydrochemical interactions in a subarctic permafrost environment, Hydrol. Proc., 31(2), 462–475, 2017.

Moskalenko, N. G.: Permafrost and vegetation changes in the Nadym region of West Siberian northern taiga due to the climate change and technogenesis, Kriosfera Zemli, 8(4), 18–23, 2009.

Moulton, K. L., West, J., Berner, R. A.: Solute flux and mineral mass balance approaches to the quantification of plant effects on silicate weathering, Am. J. Sci., 300, 539-570, 2000.

Muller, F. L. L., Chang, K.-C., Lee, C.-L. and Chapman, S. J.: Effects of temperature, rainfall and conifer felling practices on the surface water chemistry of northern peatlands, Biogeochemistry, 126, 343–362, 2015.

Natali, S. M., Schuur, E. A. G., Trucco, C., Pries, C. E. H., Crummer, K. G., and Lopez, A. F. B.: Effects of experimental warming of air, soil and permafrost on carbon balance in Alaskan tundra, Global Change Biol., 17(3), 1394-1407, DOI: 10.1111/j.1365-2486.2010.02303.x, 2011.

Natali, S. M., Schuur, E. A. G., Mauritz, M., Schade, J. D., Celis, G., Crummer, K. G., Johnston, C., Krapek, J., Pegoraro, E., Salmon, V. G., Webb, E. E., Permafrost thaw and soil moisture driving CO2 and CH4 release from upland tundra, J. Geophys. Res. – Biogeosciences, 120(3), 525-537, DOI: 10.1002/2014JG002872, 2015.

Neubauer, E., Kohler, S.J., von der Kammer, F., Laudon, H., and Hofmann, T.: Effect of pH and stream order on iron and arsenic speciation in boreal catchments, Environ. Sci. Technol., 47, 7120-7128, 2013.

Novikov, S. M., Moskvin, Y. P., Trofimov, S. A., Usova, L. I., Batuev, V. I., Tumanovskaya, S. M., Smirnova, V. P., Markov, M. L., Korotkevicth, A. E., and Potapova, T. M.: Hydrology of bog territories of the permafrost zone of western Siberia, BBM publ. House, St. Petersbourg, 535 pp., 2009 (in Russian).

Olefeldt, D., and Roulet, N. T.: Effects of permafrost and hydrology on the composition and transport of dissolved organic carbon in a subarctic peatland complex, J. Geophys. Res., 117, G01005, doi:10.1029/2011JG001819, 2012.

Olefeldt, D., Roulet, N. T., Giesler, R., and Persson, A.: Total waterborne carbon export and DOC composition from ten nested subarctic peatland catchments – importance of peatland cover, groundwater influence, and inter-annual variability of precipitation patterns, Hydrol. Process., 27, 2280–2294, 2013.

Olefeldt, D., Persson, A., and Turetsky, M. R.: Influence of the permafrost boundary on dissolved organic matter characteristics in rivers within the Boreal and Taiga plains of western Canada, Environ. Res. Lett., 9, Art No 035005, doi:10.1088/1748-9326/9/3/035005, 2014.

Ovchinnikov, S. M., Sokolova, T. A., and Targulian, V. P.: Clay minerals of clay loam soils of tundra and forest-tundra of western Siberia, Pochvovedenie (Soil Science), 12, 90–103, 1973.

Panova N. K., Antipina T. G., Gilev A.V., Trofimova S. S., Zinoviev E.V., and Erokhin N. G. Holocene dynamics of vegetation and ecological conditions in the Southern Yamal Peninsula according to the results of comprehensive analysis of a relict peat bog deposit, Russ. J. Ecol., 41(1), 20–27, DOI: 10.1134/S1067413610010042, 2010.

Pastukhov, A. V., Marchenko-Vagapova, T. I., Kaverin, D. A., and Goncharova, N. N.: Genesis and evolution of peat plateuas in the sporadic permafrost area in the European North-East (middle basin of the Kosyu river), Earth's Cryosphere, XX(1), 3–13, http://www.izdatgeo.ru/pdf/earth_cryo/2016-1/3_eng.pdf, 2016.

Pastukhov, A. V. and Kaverin, D. A.: Ecological state of peat plateaus in northeastern European Russia, Russ. J. Ecol., 47(2), 125–132, doi:10.1134/S1067413616010100, 2016.

Pavlov, A. V. and Moskalenko, N. G.: The thermal regime of soils in the north of Western Siberia, Permafrost Periglac. Proc., 13, 43–51, doi:10.1002/ppp.409, 2002.

Pokrovsky, O. S., Schott, J., and Dupre, B.: Trace element fractionation and transport in boreal rivers and soil porewaters of permafrost-dominated basaltic terrain in Central Siberia, Geochim. Cosmochim. Ac., 70, 3239–3260, 2006.

Pokrovsky, O. S., Shirokova, L. S., Kirpotin, S. N., Audry, S., Viers, J., and Dupré, B.: Effect of permafrost thawing on the organic carbon and metal speciation in thermokarst lakes of western Siberia, Biogeosciences, 8, 565-583, 2011.

Pokrovsky, O. S., Reynolds, B. C., Prokushkin, A. S., Schott, J., and Viers, J.: Silicon isotope variations in Central Siberian rivers during basalt weathering in permafrost-dominated larch forests, Chem. Geol., 355, 103–116, 2013.

Pokrovsky, O. S., Manasypov, R. M., Shirokova, L. S., Loiko, S. V., Krickov, I. V., Kopysov, S. G., et al.: Permafrost coverage, watershed area and season control of dissolved carbon and major elements in western Siberia rivers, Biogeosciences, 12, 6301–6320, 2015.

Pokrovsky, O. S., Manasypov, R. M., Loiko, S. V., Krickov, I. A., Kopysov, S. G., Kolesnichenko, L., G., Vorobyev, S. N., Kirpotin, S. N.: Trace element transport in western Siberia rivers across a permafrost gradient, Biogeosciences, 13, 1877–1900, 2016a.

Pokrovsky, O. S., Manasypov, R. M., Loiko, S. V., Shirokova, L. S.: Organic and organo-mineral colloids of discontinuous permafrost zone, Geochim. Cosmochim. Ac., 188, 1–20, 2016b.

Polishchuk, Y. M., Bogdanov, A. N., Polischuk, V. Y., Manasypov, R. M., Shiorkova, L. S., Kirpotin, S. N., Pokrovsky, O. S.: Size-distribution, surface coverage, water, carbon and metal storage of thermokarst lakes (> 0.5 ha) in permafrost zone of the Western Siberia Lowland, Water, submitted, 2016.

Ponomareva, O. E., Gravis, A. G., and Berdnikov, N. M.: Contemporary dynamics of frost mounds and flat peatlands in north taiga of West Siberia (on the example of Nadym site), Kriosfera Zemli, XVI, № 4, 21–30, 2012.

Pries, C. E. H., Schuur, E. A. G., Natali, S. M., Crummer, K. G.: Old soil carbon losses increase with ecosystem respiration in experimentally thawed tundra, Nature Clim. Change, 6(2), 214, DOI: 10.1038/NCLIMATE2830, 2016.

Prokushkin, A. S., Kajimoto, T., Prokushkin, S. G., McDowell, W. H., Abaimov, A. P., Matsura, Y.: Climatic factors influencing fluxes of dissolved organic carbon from the forest floor in a continuous-permafrost Siberian watershed, Can. J. For. Res, 35, 2130–2140, doi:10.1139/X05-150, 2005.

Prokushkin, A. S., Pokrovsky, O. S., Shirokova, L. S., Korets, M. A., Viers, J., Prokushkin, S. G., Amon, R., Guggenberger, G., and McDowell, W. H.: Sources and export fluxes of dissolved carbon in rivers draining larch-dominated basins of the Central Siberian Plateau, Environ. Res. Lett., 6, 045212, 14 pp., doi:10.1088/1748-9326/6/4/045212, 2011.

Quinton, W. L., Gray, D. M., Marsh, P.: Subsurface drainage from hummock-covered hillslope in the Arctic tundra, J. Hydrol. 237, 113–125, 2000.

Quinton, W. L., Pomeroy, J. W.: Transformations of runoff chemistry in the Arctic tundra, Northwest Territories, Canada, Hydrological Processes, 20(14), 2901–2919, doi: 10.1002/hyp.6083, 2006.

Quinton, W. L., Elliot, T., Price, J. S., Rezanezhad, F., Heck, R.: Measuring physical and hydraulic properties of peat from X-ray tomography, Geoderma 153, 269–277, 2009.

Quinton, W. L., Baltzer, J. L. : The active-layer hydrology of a peat plateau with thawing permafrost (Scotty Creek, Canada), Hydrogeol. J., 21(1), 201-220, 2013.

Raudina, T.V., Loyko, S.V., Krickov, I.V., and Lim, A.G.: Comparing the composition of soil waters of West Siberian frozen mires sampled by different methods, Vestnik Tomskogo gosudarstvennogo universiteta. Biologiya – Tomsk State University Journal of Biology, 3(35), 26-42. doi: 10.17223/19988591/35/2, 2016.

Rember, R. D., Trefry, J. H.: Increased concentrations of dissolved trace metals and organic carbon during snowmelt in rivers of the Alaskan Arctic, Geochim. Cosmochim. Ac., 68(3), 477–489, 2004.
Reynolds, B., Stevens, P. A., Hughes, S., Brittain, S. A.: Comparison of field techniques for sampling soil solution in an upland peatland, Soil Use and Management, 20(4), 454–456, doi:10.1079/SUM2004277, 2004.
Rezanezhad, F., Quinton,W. L., Price, J. S., Elrick, D., Elliot, T., Heck, R.: Examining the effect of pore size distribution and shape on flow through unsaturated peat using computed tomography, Hydrol. Earth Syst. Sci. 13, 1993–2002, 2009.
Rezanezhad, F., Quinton, W. L., Price, J. S., Elrick, D., Elliot, T., and Shook, K. R.: Influence of pore size and geometry on peat unsaturated hydraulic conductivity computed from 3D computed tomography image analysis, Hydrol. Process. 24, 2983–2994, 2010.
Rezanezhad F., Price, J.S., Quinton, W.L., Lennartz B., Milojevic, T., Van Cappellen, P.: Structure of peat soils and implications for water storage, flow and solute transport: A review update for geochemists, Chem. Geol., 429, 75–84, 2016.
Romanovsky, V. E., Drozdov, D. S., Oberman, N. G., Malkova, G. V., Kholodov, A. L., Marchenko, S. S., Moskalenko, N. G., Sergeev, D. O., Ukraintseva, N. G., Abramov, A. A., Gilichinsky, D. A., and Vasiliev, A. A.: Thermal State of Permafrost in Russia, Permafrost Periglacial Proc., 21, 136–155, 2010.
Schlotter, D., Schack-Kirchner, H., Hildebrand, E.E., von Wilpert, K.: Equivalence or complementarity of soil-solution extraction methods, J. Plant Nutr. Soil Sci., 175(2), 236-244, doi: 10.1002/jpln.201000399, 2012.
Schott, J., Pokrovsky, O. S., Oelkers, E. H.: The link between mineral dissolution/precipitation kinetics and solution chemistry, Rev. Mineral. Geochem., Thermodynamics and Kinetics of Water-Rock Interaction, 70, 207–258, 2009.
Schuur, E. A. G., McGuire, A. D., Schädel, C., Grosse, G., Harden, J. W., Hayes, D.J., Hugelius, G., Koven, C. D., Kuhry, P., Lawrence, D. M., Natali, S. M., Olefeldt, D., Romanovsky, V. E., Schaefer, K., Turetsky, M. R, Treat, C. C. and Vonk, J. E.: Climate change and the permafrost carbon feedback, Nature, 520, 171–179. doi:10.1038/nature14338, 2015.
Shevchenko, V. P., Pokrovsky, O. S., Vorobyev, S. N., Krickov, I. V., Manasypov, R. M., Politova, N. V., Kopysov, S. G., Dara, O. M., Auda, Y., Shirokova, L. S., Kolesnichenko, L. G., Zemtsov, V. A., and Kirpotin, S. N.: Impact of snow deposition on major and trace element concentrations and fluxes in surface waters of Western Siberian Lowland, Hydrol. Earth Syst. Sci. Discuss., doi:10.5194/hess-2016–578, in review, 2016.
Shirokova, L. S., Pokrovsky, O. S., Kirpotin, S. N., Desmukh, C., Pokrovsky, B. G., Audry, S., and Viers, J.: Biogeochemistry of organic carbon, $CO_2$, $CH_4$, and trace elements in thermokarst water bodies in discontinuous permafrost zones of Western Siberia, Biogeochemistry, 113, 573–593, 2013.
Shotyk, W., Bicalho, B., Cuss, C. W., Duke, M. J. M., Noernberg, T., Pelletier, R., Steinnes, E., and Zaccone, C.: Dust is the dominant source of "heavy metals" to peat moss (*Sphagnum fuscum*) in the bogs of the Athabasca Bituminous Sands region on northern Alberta, Environ. Internat., 92-93, 494-506, 2016.
Shotyk, W., Rausch, N., Nieminen, T. M., Ukonmaanaho, L., and Krachler, M.: Isotopic composition of Pb in peat and porewaters from three contrasting ombrotrophic bogs in Finland: Evidence of chemical diagenesis in rresponse to acidification, Environ. Sci. Technol., 50, 9943-9951, 2016.
Smith, L. C., Macdonald, G. M., Velichko, A. A., Beilman, D. W., Borisova, O. K., Frey, K. E., Kremenetsky, K. V., and Sheng, Y.: Siberian peatlands as a net carbon sink and global methane source since the early Holocene, Science, 303, 353–356, 2004.
Smith, L. C., Beilman, D. W., Kremenetski, K. V., Sheng, Y., MacDonald, G. M., Lammers, R. B., Shiklomanov, A. I., and Lapshina, E. D.: Influence of permafrost on water storage in West Siberian peatlands revealed from a new database of soil properties, Permafrost Periglacial Proc., 23, 69-79, 2012.
Smolyakov, B. S.: The problem of acid fallauts in the north of West Siberia, Sibirskiy Ekologicheskiy Zhurnal, 1, 21–30, 2000.
Spencer, R. G. M., Mann, P. J., Dittmar, T., Eglinton, T. I., McIntyre, C., Holmes, R. M., Zimov, N., Stubbins, A.: Detecting the signature of permafrost thaw in Arctci rivers, Geophys. Res. Lett., 42, 2830–2835, doi:10.1002/2015GL063498, 2015.
Spencer, R. G. M., Aiken, G. R., Wickland, K. P., Striegl, R. G., and Hernes, P. J.: Seasonal and spatial variability in dissolved organic matter quantity and composition from the Yukon River basin, Alaska, Global Biogeochem. Cy., 22, GB4002, doi:10.1029/2008GB003231, 2008.
Starr, M. and Ukonmaanaho, L.: Levels and Characteristics of TOC in Throughfall, Forest Floor Leachate and Soil Solution in Undisturbed Boreal Forest Ecosystems, in: Biogeochemical Investigations of Terrestrial, Freshwater, and Wetland Ecosystems across the Globe, Water, Air, and Soil Pollution, Kluwer Academic Publisher, 715–729, 2004.
Stendel, M., Christensen, J. H.: Impact of global warming on permafrost conditions in a coupled GCM, Geophys. Res. Lett., 29(13), Art No 1632, doi:10.1029/2001GL014345, 2002.

Stepanova, V. M., Pokrovsky, O. S., Viers, J., Mironycheva-Tokareva, N. P., Kosykh, N. P., and Vishnyakova, E. K.: Major and trace elements in peat profiles in Western Siberia: impact of the landscape context, latitude and permafrost coverage, Appl. Geochem., 53, 53–70, 2015.

Striegl, R. G., Aiken, G. R., Dornblaser, M. M., Raymond, P. A., and Wickland, K. P.: A decrease in discharge-normalized DOC export by the Yukon River during summer through autumn, Geophys. Res. Lett., 32, L21413, doi:10.1029/2005GL024413, 2005.

Strack , M., Waddington, J. M., Bourbonniere, R. A., Buckton, E. L., Shaw, K., Whittington, P., Price, J. S.: Effect of water table drawdown on peatland dissolved organic carbon export and dynamics, Hydrol. Proces., 22(17), 3373–3385, doi:10.1002/hyp.6931, 2008.

Stutter, M. I., Billett, M. F.: Biogeochemical controls on streamwater and soil solution chemistry in a High Arctic environment, Geoderma, 113(1–2), 127–146, doi:10.1016/S0016-7061(02)00335-X, 2003.

Syso, A. I.: Features of distribution of chemical elements in soil-forming rocks and soils of Western Siberia, Novosibirsk, Izd-vo SO RAN, 277 pp, 2007.

Swindles, G. T., Morris, P. J., Mullan, D., Watson, E. J., Turner, T. E., Roland, T. P. et al.: The long-term fate of permafrost peatlands under rapid climate warming, Scientific Reports 5, 17951, doi:10.1038/srep17951, 2015.

Tank, S. E., Lesack, L. F. W., and Hesslein, R. H.: Northern delta lakes as summertime $CO_2$ absorbers within the Arctic landscape, Ecosystems, 12, 144–157, 2009.

Tank, S. E., Frey, K. E., Striegl, R. G., Raymond, P. A., Holmes, R. M., McClelland, J. W., and Peterson, B. J.: Landscape level controls on dissolved carbon flux from diverse catchments of the circumboreal, Glob. Biogeochem. Cy., 26, GB0E02, doi:10.1029/2012GB004299, 2012a.

Tank, S. E., Raymond, P. A., Striegl, R. G., McClelland, J. W., Holmes, R. M., Fiske, G. J., and Peterson, B. J.: A land-to-ocean perspective on the magnitude, source and implication of DIC flux from major Arctic rivers to the Arctic Ocean, Global Biogeochem. Cy., 26, GB4018, doi:10.1029/2011GB004192, 2012b.

Tank, S. E., Striegl, R. G., McClelland, J. W., Kokelj, S. V.: Multi-decadal increases in dissolved organic carbon and alkalinity flux from the Mackenzie drainage basin to the Arctic Ocean, Environ. Res. Lett., 11(5), 054015. doi:10.1088/1748-9326/11/5/054015, 2016.

Tarnocai, C., Canadell, J. G., E. Schuur A. G., Kuhry P., Mazhitova G., and Zimov S.: Soil organic carbon pools in the northern circumpolar permafrost region, Global Biogeochem. Cycles, 23, GB2023, doi:10.1029/2008GB003327, 2009.

Tyrtikov, A. P.: Thawing of soils in tundra of western Siberia, in: Natural environment of western Siberia, Issue 3, Izd-vo MG, Moscow, 160–169, 1973 (in Russian).

Uyguner, C. and Bekbolet, M.: Implementation of spectroscopic parameters for practical monitoring of natural organic matter. Desalination 176, 47–55, 2005.

Van Hees, P. A. W., Lundström, U. S. and Giesler, R.: Low molecular weight organic acids and their Al-complexes in soil solutionc-compostion, distribution and seasonal variation in three podzolized soils, Geoderma 94, 173–200, 2000a.

Van Hees, P. A. W., Lundström, U. S., Starr, M. and Giesler, R.: Factors influencing aluminium concentrations in soil solution from podzols, Geoderma 94, 289–310, 2000b.

Vasyukova, E.V., Pokrovsky, O.S., Viers, J., Oliva, P., Dupré, B., Martin, F., and Candadaup, F.: Trace elements in organic- and iron-rich surficial fluids of the boreal zone: Assessing colloidal forms via dialysis and ultrafiltration, Geochim. Cosmochim. Acta, 74, 449-468, 2010.

Vasiliev, A. A., Streletskaya, I. D., Shirokov, R. S., and Oblogov, G. E.: Evolution of cryolithozone of coastal zone of western Yamal during climate change, Kriosfera Zemli, 2, 56–64, 2011 (in Russian).

Vonk, J. E., Tank, S. E., Mann, P. J., Spencer, R. G. M., Treat, C. C., Striegl, R. G., Abbott, B. W., and Wickland, K. P.: Biodegradability of dissolved organic carbon in permafrost soils and aquatic systems: a meta-analysis, Biogeosciences, 12, 6915–6930, doi:10.5194/bg-12-6915-2015, 2015a.

Vonk, J. E., Tank, S. E., Bowden, W. B., Laurion, I., Vincent, W. F., Alekseychik, P., Amyot, M., Billet, M. F., Canário, J., Cory, R. M., Deshpande, B. N., Helbig, M., Jammet, M., Karlsson, J., Larouche, J., MacMillan, G., Rautio, M., Walter Anthony, K. M., Wickland, K. P.: Reviews and syntheses: Effects of permafrost thaw on Arctic aquatic ecosystems, Biogeosciences, 12, 7129–7167, doi:10.5194/bg-12-7129-2015, 2015b.

Walvoord, M. A. and Kurylyk, B. L.: Hydrological impacts of thawing permafrost – a review, Vadoze Zone J., 15(6), doi: 10.2136/vzj2016.01.0010, 2016.

Ward, C. P. and Cory, R. M.: Chemical composition of dissolved organic matter draining permafrost soils, Geochim. Cosmochim. Ac., 167, 63–79, doi:10.1016/j.gca.2015.07.001, 2015.

Weishaar, J. L., Aiken, G. R., Bergamaschi, B. A., Fram, M. S., Fujii, R., and Mopper, K. (2003) Evaluation of specific ultraviolet absorbance as an indicator of the chemical composition and reactivity of dissolved organic carbon, Env. Sci. Technol., 37, 4702–4708, 2003.

Wickland, K. P., Aiken, G. R., Butler, K., Dornblaser, M. M., Spencer, R. G. M., and Striegl, R. G.: Biodegradability of dissolved organic carbon in the Yukon River and its tributaries: Seasonality and importance of inorganic nitrogen, Global Biogeochem. Cycles, 26, GB0E03, doi:10.1029/2012GB004342, 2012.

Working Group WRB: World Reference Base for Soil Resources 2014, International soil classification system for naming soils and creating legends for soil maps, World Soil Resources Reports, 106, FAO, Rome, 2014.

Yang, Z., Wullschleger, S. D., Liang, L., Graham, D. E., Gu, B.: Effects of warming on the degradation and production of low-molecular-weight labile organic carbon in an Arctic tundra soil, Soil Biol. Biochem., 95, 202–211, doi:10.1016/j.soilbio.2015.12.022, 2016.

Yang, D., Ye, B., and Shiklomanov, A.: Discharge characteristics and changes over the Ob River watershed in Siberia, J. Hydrometeorol., 5, 595–610, 2004.

Yeghicheyan, D., Bossy, C., Bouhnik Le Coz, M., Douchet, Ch., Granier, G., Heimburger, A., Lacan, F., Lanzanova, A., Rousseau, T. C. C., Seidel, J.-L., Tharaud, M., Candaudap, F., Chmeleff, J., Cloquet, C., Delpoux, S., Labatut, M., Losno, R., Pradoux, C., Sivry, Y., and Sonke, J. E.: A Compilation of Silicon, Rare Earth Element and Twenty-One other Trace Element Concentrations in the Natural River Water Reference Material SLRS-5 (NRC-CNRC), Geostand. Geoanal. Res., 37, 449–467, doi:10.1111/j.1751-908X.2013.00232.x, 2013.

Zhang, T. J., Frauenfeld, O. W., Serreze, M. C., Etringer, A., Oelke, C., McCreight, J., Barry, R. G., Gilichinsky, D., Yang, D. Q., Ye, H. C., Ling, F. and Chudinova, S.: Spatial and temporal variability in active layer thickness over the Russian Arctic drainage basin, J. Geophys. Res.-Atmospheres, 110, doi:10.1029/2004JD005642, 2005.

Table 1. Physico-geographical, permafrost and soil parameters of 5 study sites.

| Site | Latitude, °N | MAT, °C | Mean annual precipitation, mm | Mineral substrate | Micro-landscapes | Peat thickness, m | Seasonal thaw depth, cm | Soil type (WRB, 2014) |
|---|---|---|---|---|---|---|---|---|
| Tazovsky, (Tz) | 67.4 | –9.1°C | 363 | Clay loam and loam | polygon | 2.0–4.0 | 41 | Dystric Hemic Epicryic Histosols (Hyperorganic); Dystric Murshic Hemic Epicryic Histosols (Hyperorganic) |
| | | | | | permafrost subsidences | | 55 | Dystric Epifibric Hemic Cryic Histosols (Hyperorganic) |
| | | | | | frost crack | | 44 | Dystric Epifibric Cryic Histosols (Hyperorganic) |
| | | | | | hollows | 0.2–1.5 | 65 | Dystric Fibric Cryic Histosols; Histic Reductaquic Cryosols (Clayic) |
| Urengoy, (Ur) | 66.1 | –7.8°C | 453 | Loam and silt loam | peat mounds | 2.0–2.5 | 49 | Dystric Hemic Epicryic Histosols (Hyperorganic) |
| | | | | | hollows | 0.3–1.2 | 98 | Histic Reductaquic Cryosols (Loamic); Dystric Fibric Histosols (Gelic) |
| Pangody, (Pg) | 65.9 | –6.4°C | 484 | Loam | peat mounds | 0.2–1.3 | 49 | Dystric Hemic Epicryic Histosols; Histic Cryosols (Loamic); Histic Oxyaquic Turbic Cryosols (Loamic) |
| | | | | | permafrost subsidences | 0.6–1.1 | 74 | Dystric Hemic Endocryic Histosols |
| | | | | | hollows | 0.3–1.0 | 82 | Dystric Epifibric Endocryic Histosols; Histic Reductaquic Turbic Cryosols (Loamic); Dystric Fibric Histosols (Gelic) |
| Khanymey, (Kh) | 63.8 | –5.6°C | 540 | Sand | peat mounds | 0.1–1.4 | 90 | Dystric Hemic Cryic Histosols; Spodic Histic Turbic Cryosols (Albic, Arenic); Histic Turbic Cryosols (Albic, Arenic) |
| | | | | | permafrost subsidences | 0.7–1.1 | 165 | Dystric Hemic Histosols (Gelic) |
| | | | | | hollows | 0.4–1.1 | 215 | Dystric Epifibric Histosols; Spodic Histic Turbic Cryosols (Arenic); Gleyic Histic Entic Podzols (Turbic) |
| Kogalum, (Kg) | 62.3 | –4.0°C | 594 | Sand | ridge | 1.7–2.3 | – | Dystric Ombric Fibric Histosols (Hyperorganic) |
| | | | | | hollows | 1.0–1.5 | – | Dystric Ombric Fibric Histosols |

**Table 2.** Mean values of DOC, major and TE concentration with S.D. of elements in various microlandscape across the permafrostgradient. Concentrations of DOC, DIC, $Cl^-$, $SO_4^{2-}$, Ca, Mg, K, Al, Fe, Si, and Na are given in ppm and all other trace elements are in ppb.

| Elements | Kogalym (62.259°N) | | Khanymey (63.785°N) | | | Pangody (65.873°N) | | Urengoy (66.085°N) | | | Tazovsky (67.367°N) | | | WSL-mean mound/ poligon | WSL mean hollow |
|---|---|---|---|---|---|---|---|---|---|---|---|---|---|---|---|
| | mound n=4 | hollow n=2 | mound n=20 | hollow n=4 | subsidence n=4 | mound n=8 | hollow n=4 | mound n=3 | hollow n=4 | subsidence n=2 | poligon n=12 | hollow n=7 | frost crack n=4 | | |
| DOC | 50.56±15.6 | 33.7±4.1 | 82.9±29.7 | 49.6±13.5 | 76.5±21 | 90.2±55.3 | 81.58±15 | 74.28±25.2 | 50.2±3.64 | 97.9±19.9 | 72.9±12.9 | 52.53±7.7 | 58.4±30.8 | 79.8 | 58.1 |
| DIC | 1.45±0.27 | 1.42±0.3 | 1.65±0.36 | 1.42±0.05 | 1.7±0.11 | 1.84±0.35 | 1.54±0.46 | 1.36±0.17 | 1.58±0.7 | 1.32±0.17 | 1.44±0.18 | 1.68±0.13 | 1.76±0.42 | 1.59 | 1.56 |
| $Cl^-$ | 0.61±0.5 | 0.91±0.06 | 0.49±0.4 | 0.26±0.17 | 0.31±0.16 | 0.52±0.43 | 0.68±0.45 | 0.47±0.33 | 0.54±0.41 | 0.53±0.21 | 0.20±0.18 | 0.18±0.09 | 0.28±0.15 | 0.42 | 0.43 |
| $SO_4^{2-}$ | 0.13±0.03 | 0.16±0.09 | 0.64±0.47 | 0.15±0.02 | 0.14±0.06 | 0.41±0.35 | 0.24±0.18 | 0.81±0.14 | 0.16±0.05 | 0.17±0.03 | 0.60±0.44 | 0.067±0.04 | 0.13±0.10 | 0.56 | 0.14 |
| Ca | 1.03±0.34 | 1.07±0.57 | 0.74±0.52 | 1.34±0.17 | 0.97±0.14 | 1.33±0.4 | 1.14±0.16 | 1.13±0.22 | 1.17±0.35 | 0.97±0.17 | 2.04±1.7 | 1.78±1.03 | 1.8±0.4 | 1.31 | 1.40 |
| Mg | 0.13±0.07 | 0.12±0.05 | 0.14±0.11 | 0.21±0.09 | 0.13±0.04 | 0.28±0.22 | 0.35±0.27 | 0.12±0.03 | 0.19±0.18 | 0.07±0.001 | 0.3±0.29 | 0.34±0.3 | 0.36±0.16 | 0.20 | 0.27 |
| K | 1.06±0.49 | 1.16±0.26 | 0.32±0.13 | 0.34±0.26 | 0.31±0.06 | 0.99±0.62 | 0.79±0.33 | 0.21±0.06 | 0.16±0.05 | 0.18±0.004 | 0.26±0.17 | 0.19±0.06 | 0.14±0.1 | 0.47 | 0.42 |
| Al | 0.13±0.06 | 0.15±0.03 | 0.19±0.12 | 0.26±0.04 | 0.20±0.05 | 0.39±0.26 | 0.67±0.33 | 0.31±0.15 | 0.18±0.05 | 0.17±0.03 | 0.41±0.3 | 0.37±0.22 | 0.42±0.22 | 0.28 | 0.35 |
| Fe | 1.17±1.04 | 0.96±0.6 | 0.54±0.42 | 0.76±0.21 | 0.85±0.19 | 1.97±1.05 | 1.99±1.23 | 0.90±0.04 | 1.54±0.6 | 0.87±0.13 | 1±0.73 | 1.14±0.65 | 2.19±0.97 | 0.99 | 1.28 |
| Si | 1.94±1.45 | 1.12±0.33 | 1.04±1.27 | 0.6±0.18 | 0.82±0.32 | 2.94±1.44 | 3.08±1.7 | 0.49±0.14 | 0.82±0.38 | 0.38±0.03 | 1.12±0.97 | 1.27±1.35 | 1.77±1.51 | 1.39 | 1.42 |
| Li | 0.46±0.04 | 0.63±0.10 | 0.45±0.42 | 0.39±0.05 | 0.40±0.20 | 1.14±0.76 | 1.11±0.63 | 0.17±0.01 | 0.37±0.36 | 0.17±0.01 | 0.36±0.15 | 0.80±0.71 | 0.44±0.25 | 0.53 | 0.68 |
| B | 1.39±0.57 | 3.39±0.07 | 4.09±2.02 | 2.97±0.97 | 2.91±1.99 | 2.19±1.29 | 2.03±1.16 | 0.63±0.34 | N.D. | N.D. | 3.54±1.52 | 1.31±0.71 | 2.38±0.85 | 3.26 | 2.13 |
| Na | 0.44±0.25 | 0.45±0.09 | 0.28±0.12 | 0.35±0.15 | 0.26±0.03 | 0.39±0.2 | 0.50±0.11 | 0.23±0.1 | 0.25±0.22 | 0.14±0.02 | 0.19±0.08 | 0.26±0.10 | 0.20±0.1 | 0.29 | 0.34 |
| Ti | 2.33±1.21 | 0.66±0.21 | 2.92±2.02 | 2.02±0.48 | 3.23±0.8 | 3.8±1.57 | 3.68±1.58 | 1.72±0.36 | 1.38±0.32 | 1.43±0.02 | 3.69±0,71 | 3.48±1.34 | 5.25±2.78 | 3.07 | 2.54 |
| V | 0.51±0.38 | 0.28±0.18 | 0.43±0.26 | 0.35±0.22 | 0.56±0.114 | 0.67±0.22 | 0.96±0.67 | 0.77±0.47 | 0.26±0.082 | 0.28±0.09 | 1.71±1.51 | 0.97±0.52 | 1.63±0.99 | 0.83 | 0.65 |
| Cr | 0.54±0.28 | 0.31±0.11 | 1.12±0.36 | 1.17±0.56 | 1.23±0.42 | 1.12±0.4 | 1.34±0.39 | 0.27±0.18 | 0.39±0.2 | 0.203±0.001 | 0.93±0.38 | 0.86±0.31 | 1.22±0.65 | 0.97 | 0.87 |
| Mn | 6.89±3.3 | 10.8±0.4 | 3.33±2.95 | 3.05±1.6 | 2.64±1.34 | 11.3±8.5 | 5.77±4.25 | 6.05±2.02 | 14.38±5.54 | 9.31±1.58 | 58.9±37.3 | 47.3±40.0 | 59.1±34.33 | 19.7 | 21.21 |
| Co | 0.18±0.04 | 0.16±0.12 | 0.22±0.11 | 0.29±0.1 | 0.34±0.09 | 1.18±0.54 | 1.24±0.65 | 0.26±0.09 | 0.34±0.14 | 0.21±0.03 | 0.99±0.63 | 0.92±0.62 | 1.43±0.46 | 0.59 | 0.677 |
| Ga | 0.05±0.04 | 0.02±0.01 | 0.51±0.45 | 0.06±0.02 | 0.55±0.44 | 0.07±0.03 | 0.15±0.15 | 0.59±0.22 | 0.42±0.18 | 0.32±0.01 | 0.20±0.18 | 0.31±0.23 | 0.51±0.42 | 0.32 | 0.224 |
| As | 1.00±0.49 | 0.76±0.2 | 0.53±0.31 | 0.96±0.3 | 0.74±0.32 | 0.83±0.6 | 1.07±0.86 | 0.2±0.06 | 0.17±0.06 | 0.105±0.075 | 1.12±0.98 | 0.96±0.37 | 1.90±0.89 | 0.76 | 0.796 |
| Rb | 0.93±0.53 | 0.35±0.2 | 0.48±0.36 | 0.62±0.31 | 0.47±0.46 | 0.72±0.58 | 0.33±0.17 | 0.23±0.22 | 0.27±0.15 | 0.056±0.035 | 0.37±0.28 | 0.56±0.50 | 0.53±0.26 | 0.52 | 0.454 |
| Zr | 0.10±0.10 | 0.02±0.001 | 0.21±0.23 | 0.13±0.06 | 0.24±0.15 | 0.33±0.23 | 0.56±0.3 | 0.14±0.06 | 0.19±0.2 | 0.066±0.050 | 0.54±0.45 | 0.34±0.15 | 0.53±0.24 | 0.304 | 0.281 |
| Nb | 0.01±0.005 | 0.003±0.002 | 0.013±0.009 | 0.017±0.009 | 0.011±0.003 | 0.021±0.01 | 0.026±0.016 | 0.004±0.002 | 0.004±0.001 | 0.004±0.000 | 0.018±0.012 | 0.012±0.005 | 0.02±0.01 | 0.014 | 0.013 |
| Mo | 0.037±0.02 | 0.084±0.08 | 0.09±0.07 | 0.129±0.09 | 0.11±0.01 | 0.082±0.06 | 0.075±0.036 | 0.028±0.016 | 0.028±0.008 | 0.024±0.004 | 0.064±0.021 | 0.054±0.021 | 0.12±0.08 | 0.075 | 0.070 |
| Cd | 0.19±0.035 | 0.4±0.18 | 0.34±0.54 | 0.42±0.42 | 0.56±0.5 | 0.27±0.27 | 0.13±0.04 | 0.040.019 | 0.025±0.008 | 0.008±0.004 | 0.067±0.065 | 0.04±0.027 | 0.09±0.07 | 0.223 | 0.161 |
| Ni | 1.04±0.76 | 0.55±0.24 | 0.92±0.48 | 1.51±0.62 | 1.22±0.62 | 3.29±1.26 | 3.12±1.32 | 1.43±0.7 | 1.25±0.45 | 1±0.14 | 2.9±1.95 | 2.12±0.95 | 3.53±1.54 | 1.89 | 1.859 |
| Cu | 4.44±2.7 | 2.21±0.48 | 5.36±3.74 | 1.62±0.14 | 4.27±3.46 | 5.02±3.7 | 5.78±3.95 | 6.02±4 | 5.41±2.24 | 1.82±0.23 | 5.86±3.1 | 4.05±3.05 | 2.33±0.95 | 5.39 | 4.000 |
| Zn | 9.97±6.7 | 12.48±0.5 | 7.97±4.47 | 10.16±6.4 | 10.03±6.67 | 8.14±5.4 | 3.51±0.49 | 8±5.38 | 6.34±2.04 | 1.76±0.11 | 6.34±3.32 | 7.88±3.46 | 5.77±0.36 | 7.75 | 7.626 |
| Sr | 5.37±1.05 | 4.46±3.03 | 7.62±4.42 | 8.15±2.94 | 7.87±1.08 | 10.95±2.98 | 10.7±5.35 | 5.9±2.3 | 6.5±3.6 | 4.32±0.15 | 13.1±9.02 | 8.41±3.49 | 11.7±4.22 | 9.42 | 8.312 |
| Sb | 0.06±0.04 | 0.05±0.01 | 0.05±0.03 | 0.06±0.02 | 0.042±0.016 | 0.05±0.03 | 0.037±0.011 | 0.013±0.012 | 0.013±0.004 | 0.004±0.001 | 0.032±0.01 | 0.025±0.012 | 0.032±0.01 | 0.044 | 0.034 |
| Cs | 0.032±0.03 | 0.02±0.016 | 0.036±0.028 | 0.03±0.02 | 0.04±0.03 | 0.023±0.02 | 0.018±0.01 | 0.004±0.002 | 0.006±0.004 | 0.003±0.001 | 0.012±0.013 | 0.006±0.007 | 0.056±0.03 | 0.025 | 0.015 |
| Ba | 22.5±9.3 | 18.87±9.57 | 35.7±20.6 | 33.57±22.24 | 32.5±17.7 | 22.7±13.2 | 38.8±17.7 | 18.76±6.89 | 13.83±6.35 | 10.8±0.6 | 16.77±6.85 | 16.30±5.82 | 14.99±9.11 | 26.23 | 23.64 |
| La | 0.24±0.19 | 0.15±0.04 | 0.37±0.33 | 0.25±0.17 | 0.26±0.06 | 0.348±0.208 | 0.502±0.277 | 0.354±0.26 | 0.14±0.07 | 0.112±0.05 | 0.34±0.17 | 0.23±0.10 | 0.40±0.22 | 0.346 | 0.261 |
| Ce | 0.51±0.47 | 0.22±0.11 | 0.67±0.51 | 0.53±0.44 | 0.54±0.09 | 0.725±0.484 | 1.039±0.536 | 0.66±0.53 | 0.29±0.136 | 0.236±0.1 | 0.74±0.35 | 0.51±0.21 | 0.87±0.58 | 0.685 | 0.543 |
| Pr | 0.03±0.02 | 0.015±0.014 | 0.082±0.06 | 0.059±0.057 | 0.066±0.014 | 0.08±0.06 | 0.114±0.05 | 0.05±0.034 | 0.028±0.013 | 0.022±0.01 | 0.094±0.05 | 0.06±0.032 | 0.108±0.073 | 0.079 | 0.059 |

| | | | | | | | | | | | | | | | |
|---|---|---|---|---|---|---|---|---|---|---|---|---|---|---|---|
| Nd | 0.257±0.2 | 0.088±0.04 | 0.33±0.26 | 0.26±0.21 | 0.27±0.06 | 0.34±0.22 | 0.383±0.097 | 0.194±0.13 | 0.115±0.054 | 0.086±0.037 | 0.407±0.24 | 0.24±0.13 | 0.43±0.28 | 0.338 | 0.233 |
| Sm | 0.028±0.01 | 0.01±0.0074 | 0.07±0.05 | 0.044±0.038 | 0.058±0.016 | 0.072±0.047 | 0.080±0.021 | 0.04±0.027 | 0.025±0.012 | 0.018±0.009 | 0.092±0.057 | 0.052±0.031 | 0.099±0.069 | 0.071 | 0.047 |
| Eu | 0.011±0.01 | 0.004±0.002 | 0.015±0.010 | 0.010±0.007 | 0.015±0.007 | 0.015±0.01 | 0.016±0.005 | 0.012±0.006 | 0.008±0.004 | 0.007±0.003 | 0.022±0.013 | 0.013±0.008 | 0.025±0.016 | 0.017 | 0.011 |
| Gd | 0.03±0.014 | 0.02±0.007 | 0.07±0.05 | 0.05±0.05 | 0.061±0.02 | 0.069±0.046 | 0.078±0.021 | 0.042±0.027 | 0.025±0.013 | 0.019±0.009 | 0.096±0.061 | 0.052±0.029 | 0.099±0.068 | 0.0721 | 0.049 |
| Tb | 0.007±0.006 | 0.003±0.001 | 0.014±0.004 | 0.007±0.006 | 0.009±0.003 | 0.01±0.007 | 0.012±0.004 | 0.006±0.004 | 0.003±0.002 | 0.003±0.001 | 0.014±0.01 | 0.0074±0.004 | 0.015±0.011 | 0.0123 | 0.007 |
| Dy | 0.04±0.04 | 0.017±0.002 | 0.061±0.05 | 0.041±0.034 | 0.05±0.016 | 0.055±0.037 | 0.081±0.04 | 0.031±0.02 | 0.018±0.009 | 0.016±0.009 | 0.078±0.05 | 0.0424±0.026 | 0.087±0.068 | 0.0608 | 0.042 |
| Ho | 0.008±0.007 | 0.003±0.001 | 0.011±0.008 | 0.011±0.01 | 0.009±0.003 | 0.011±0.007 | 0.012±0.003 | 0.007±0.004 | 0.004±0.002 | 0.004±0.002 | 0.016±0.011 | 0.009±0.005 | 0.018±0.014 | 0.0115 | 0.008 |
| Er | 0.021±0.019 | 0.0069±0.0057 | 0.030±0.021 | 0.023±0.022 | 0.03±0.01 | 0.031±0.021 | 0.034±0.009 | 0.017±0.01 | 0.012±0.008 | 0.009±0.004 | 0.047±0.035 | 0.0261±0.016 | 0.051±0.037 | 0.0330 | 0.022 |
| Tm | 0.0028±0.0025 | 0.0015±0.00001 | 0.005±0.004 | 0.0032±0.003 | 0.004±0.001 | 0.004±0.003 | 0.005±0.001 | 0.002±0.001 | 0.002±0.001 | 0.001±0.0004 | 0.007±0.005 | 0.0035±0.003 | 0.007±0.004 | 0.0047 | 0.003 |
| Yb | 0.0164±0.014 | 0.006±0.0047 | 0.021±0.014 | 0.018±0.018 | 0.022±0.009 | 0.026±0.017 | 0.029±0.007 | 0.014±0.008 | 0.012±0.01 | 0.007±0.004 | 0.043±0.032 | 0.0250±0.017 | 0.046±0.032 | 0.0271 | 0.020 |
| Lu | 0.0022±0.0018 | 0.0014±0.00001 | 0.0034±0.003 | 0.003±0.0025 | 0.003±0.001 | 0.004±0.002 | 0.004±0.001 | 0.002±0.001 | 0.002±0.001 | 0.001±0.0004 | 0.007±0.005 | 0.0036±0.003 | 0.006±0.004 | 0.0041 | 0.003 |
| Hf | 0.004±0.003 | 0.0013±0.0002 | 0.006±0.005 | 0.008±0.003 | 0.008±0.004 | 0.012±0.008 | 0.016±0.007 | 0.006±0.003 | 0.005±0.005 | 0.003±0.002 | 0.015±0.014 | 0.011±0.005 | 0.016±0.008 | 0.0095 | 0.009 |
| W | 0.028±0.02 | 0.01±0.0006 | 0.036±0.03 | 0.039±0.031 | 0.044±0.007 | 0.026±0.015 | 0.032±0.012 | 0.008±0.007 | 0.004±0.006 | 0.001±0.001 | 0.014±0.008 | 0.015±0.006 | 0.022±0.018 | 0.0262 | 0.020 |
| Tl | 0.011±0.008 | 0.005±0.003 | 0.007±0.004 | 0.005±0.004 | 0.007±0.002 | 0.008±0.004 | 0.009±0.007 | 0.001±0.001 | 0.002±0.001 | 0.0009±0.00. | 0.003±0.001 | 0.003±0.002 | 0.006±0.003 | 0.0059 | 0.005 |
| Pb | 1.24±0.64 | 0.59±0.06 | 1.08±0.71 | 1.03±0.47 | 0.90±0.25 | 0.70±0.32 | 0.777±0.22 | 0.49±0.42 | 0.27±0.13 | 0.13±0.0015 | 0.603±0.186 | 0.666±0.348 | 0.86±0.16 | 0.8636 | 0.674 |
| Th | 0.04±0.035 | 0.015±0.006 | 0.065±0.06 | 0.040±0.035 | 0.051±0.004 | 0.08±0.04 | 0.089±0.023 | 0.073±0.053 | 0.032±0.023 | 0.02±0.007 | 0.093±0.054 | 0.049±0.024 | 0.07±0.03 | 0.0740 | 0.049 |
| U | 0.02±0.018 | 0.014±0.008 | 0.0303±0.03 | 0.026±0.02 | 0.026±0.005 | 0.028±0.016 | 0.055±0.025 | 0.008±0.006 | 0.015±0.01 | 0.005±0.001 | 0.026±0.014 | 0.021±0.018 | 0.032±0.017 | 0.0265 | 0.026 |

1039 **Table 3.** Latitudinal trends of average element concentration in two main habitats persisting in all
1040 five study sites. L is for latitude (°N) and $R^2$ is a linear regression coefficient (Eqn. 1)

| Element | Habitat | Equation | $R^2$ |
|---|---|---|---|
| S.C. | Hollow | [S.C.] = -2.367L + 207.36 | 0.15 |
| | Mound/polygon | [S.C.] = -0.493L + 73.345 | 0.006 |
| pH | Hollow | [pH] = 0.0278L + 2.4126 | 0.035 |
| | Mound/polygon | [pH] = 0.0663L - 0.3568 | 0.515 |
| DOC | Hollow | [DOC] = 4.6937L - 251.92 | 0.31 |
| | Mound/polygon | [DOC] = 4.0364L - 188.61 | 0.29 |
| SUVA | Hollow | [SUVA] = 0.148L – 6.861 | 0.599 |
| | Mound/polygon | [SUVA] = 0.0258L + 1.192 | 0.031 |
| DIC | Hollow | [DIC] = 0.0405L - 1.131 | 0.58 |
| | Mound/polygon | [DIC] = 0.0191 L + 0.3357 | 0.1 |
| $Cl^-$ | Hollow | $[Cl^-]$ = -0.084L + 5.9763 | 0.33 |
| | Mound/polygon | $[Cl^-]$ = -0.0601L + 4.368 | 0.64 |
| $SO_4^{2-}$ | Hollow | $[SO_4^{2-}]$ = -0.0087L + 0.7179 | 0.079 |
| | Mound/polygon | $[SO_4^{2-}]$ = 0.0824L - 4.8422 | 0.41 |
| Ca | Hollow | [Ca] = 0.0612L - 2.6683 | 0.19 |
| | Mound/polygon | [Ca] = 0.1828L - 10.639 | 0.59 |
| Mg | Hollow | [Mg] = 0.0405L - 2.395 | 0.69 |
| | Mound/polygon | [Mg] = 0.0302L - 1.773 | 0.43 |
| Na | Hollow | [Na] = -0.0348L + 2.621 | 0.49 |
| | Mound/polygon | [Na] = -0.0389L + 2.836 | 0.52 |
| K | Hollow | [K] = -0.1488L + 10.224 | 0.47 |
| | Mound/polygon | [K] = -0.1159L + 8.119 | 0.33 |
| Al | Hollow | [Al] = 0.0555L - 3.3573 | 0.43 |
| | Mound/polygon | [Al] = 0.0577L - 3.4737 | 0.91 |
| Fe | Hollow | [Fe] = 0.1585L - 9.109 | 0.44 |
| | Mound/polygon | [Fe] = 0.1399L - 7.934 | 0.3 |
| Ti | Hollow | [Ti] = 0.462L - 27.841 | 0.52 |
| | Mound/polygon | [T] = 0.172L - 8.3533 | 0.19 |
| Mn | Hollow | [Mn] = 5.6454L - 351.11 | 0.41 |
| | Mound/polygon | [Mn] = 7.6632L - 481.39 | 0.44 |
| Co | Hollow | [Co] = 0.1618L - 9.9304 | 0.51 |
| | Mound/polygon | [Co] = 0.1658L - 10.218 | 0.5 |
| Ni | Hollow | [Ni] = 0.3096L - 18.437 | 0.43 |
| | Mound/polygon | [Ni] = 0.4012L - 24.19 | 0.55 |
| Cu | Hollow | [Cu] = 0.6695L - 39.754 | 0.54 |
| | Mound/polygon | [Cu] = 0.2503L - 10.948 | 0.63 |
| Zn | Hollow | [Zn] = -1.2677L + 90.571 | 0.56 |
| | Mound/polygon | [Zn] = -0.5584L + 44.424 | 0.78 |
| V | Hollow | [V] = 0.1308L - 7.9299 | 0.56 |
| | Mound/polygon | [V] = 0.2026L - 12.383 | 0.6 |
| Ga | Hollow | [Ga] = 0.0686L - 4.275 | 0.68 |
| | Mound/polygon | [Ga] = 0.0207L - 1.0605 | 0.03 |
| Rb | Hollow | [Rb] = -0.0229L + 1.939 | 0.11 |
| | Mound/polygon | [Rb] = -0.096L + 6.7962 | 0.48 |
| Cs | Hollow | [Cs] = -0.0036L + 0.2517 | 0.39 |
| | Mound/polygon | [Cs] = -0.0052L + 0.361 | 0.62 |
| Sr | Hollow | [Sr] = 0.7681L - 42.186 | 0.45 |
| | Mound/polygon | [Sr] = 1.2825L - 74.614 | 0.69 |
| Zr | Hollow | [Zr] = 0.0714L - 4.399 | 0.49 |
| | Mound/polygon | [Zr] = 0.0664L - 4.0544 | 0.57 |
| Mo | Hollow | [Mo] = -0.0116L + 0.8297 | 0.4 |
| | Mound/polygon | [Mo] = 0.0011L - 0.0092 | 0.01 |
| Sb | Hollow | [Sb] = -0.0068L+ 0.4819 | 0.53 |
| | Mound/polygon | [Sb] = -0.0069L + 0.489 | 0.54 |
| Cd | Hollow | [Cd] = -0.0919L + 6.1957 | 0.79 |
| | Mound/polygon | [Cd ]= -0.0402L + 2.8027 | 0.4 |
| La | Hollow | [La] = 0.0228L - 1.224 | 0.11 |
| | Mound/polygon | [La] = 0.0163L - 0.728 | 0.42 |
| Ce | Hollow | [Ce] = 0.0675L - 3.873 | 0.19 |

| | | | |
|---|---|---|---|
| | Mound/polygon | [Ce] = 0.0387L - 1.8553 | 0.76 |
| Sm | Hollow | [Sm] = 0.0077L - 0.4591 | 0.34 |
| | Mound/polygon | [Sm] = 0.0084L - 0.4861 | 0.43 |
| Eu | Hollow | [Eu] = 0.0017L - 0.1001 | 0.56 |
| | Mound/polygon | [Eu] = 0.0015L - 0.0848 | 0.52 |
| Gd | Hollow | [Gd] = 0.0054L - 0.3021 | 0.24 |
| | Mound/polygon | [Gd] = 0.0094L - 0.5536 | 0.47 |
| Pr | Hollow | [Pr] = 0.008L - 0.4652 | 0.18 |
| | Mound/polygon | [Pr] = 0.0084L - 0.4788 | 0.46 |
| Dy | Hollow | [Dy] = -0.0003L + 0.0475 | 0.0004 |
| | Mound/polygon | [Dy] = -0.0057L + 0.41 | 0.4 |
| Yb | Hollow | [Yb] = 0.0032L - 0.189 | 0.49 |
| | Mound/polygon | [Yb] = 0.0038L - 0.2209 | 0.45 |
| Lu | Hollow | [Lu] = 0.0004L - 0.0202 | 0.39 |
| | Mound/polygon | [Lu] = 0.0006L - 0.0349 | 0.44 |
| W | Hollow | [W] = -0.0015L + 0.1214 | 0.049 |
| | Mound/polygon | [W] = -0.0038L + 0.2672 | 0.47 |
| Tl | Hollow | [Tl] = -0.0004L + 0.0327 | 0.11 |
| | Mound/polygon | [Tl] = -0.0015L + 0.1056 | 0.66 |
| Hf | Hollow | [Hf] = 0.0019L - 0.1135 | 0.47 |
| | Mound/polygon | [Hf] = 0.002L - 0.1187 | 0.68 |
| Pb | Hollow | [Pb] = -0.0438L + 3.5297 | 0.12 |
| | Mound/polygon | [Pb] = -0.1482L + 10.465 | 0.87 |
| Th | Hollow | [Th] = 0.0078L - 0.4603 | 0.34 |
| | Mound/polygon | [Th] = 0.0095L - 0.5465 | 0.92 |
| U | Hollow | [U] = 0.0021L - 0,1101 | 0.065 |
| | Mound/polygon | [U] = -0.0004L + 0,047 | 0.01 |

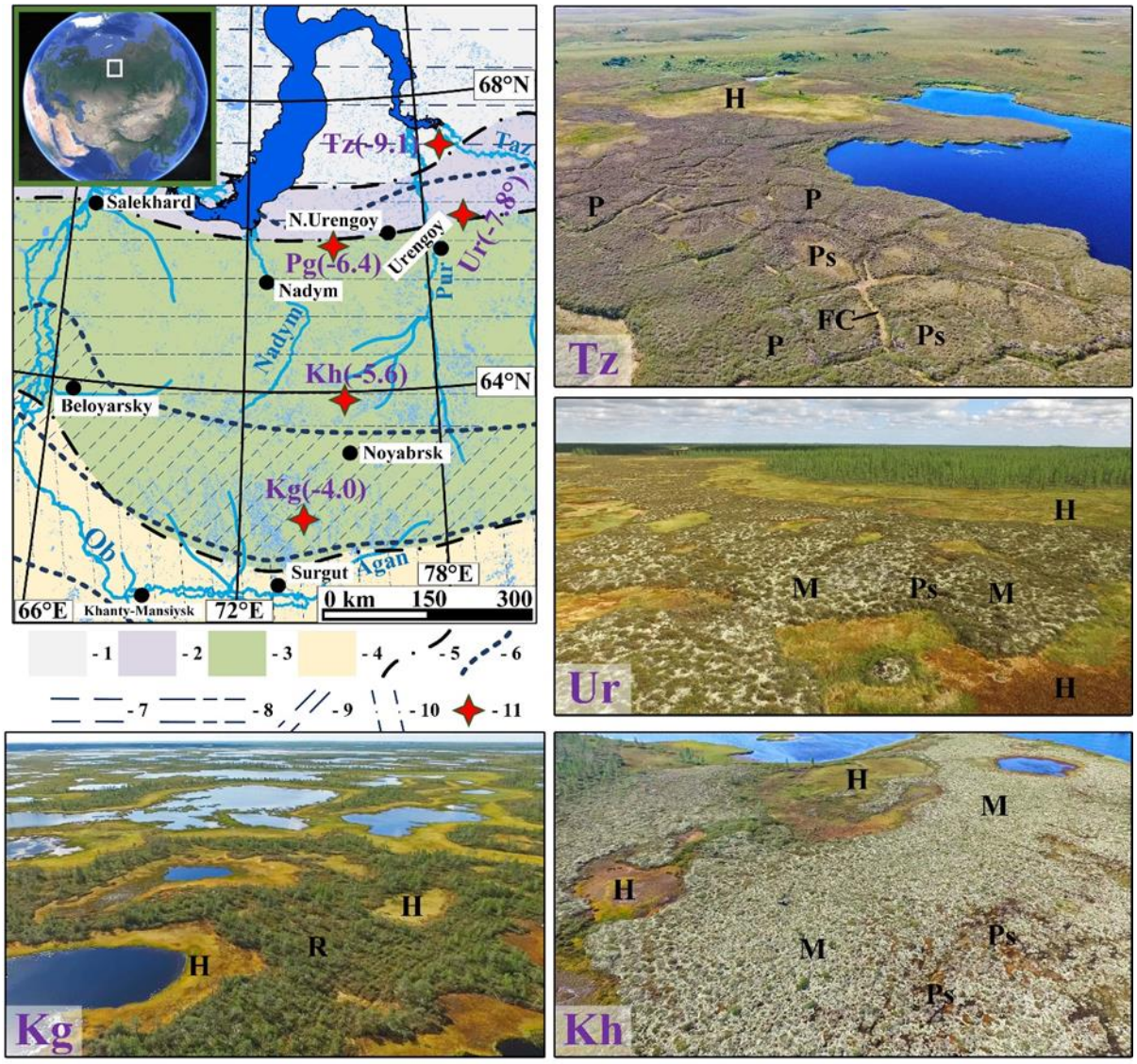


**Figure 1.** Map of the study site with permafrost boundaries (Brown et al., 2001; http://portal.inter-map.com (NSIDC)), with 5 main test sites: Kogalym (Kg), Khanymey (Kh), Pangody (Pg), Urengoy (Ur) and Tazovsky (Tz). The mean annual temperatures are given in parenthesis. The inserts represent aerial (drone-made) photos of main sites with the position of mound/polygon (M/P), hollow (H), frost crack (FC) and permafrost subsidence (Ps). On the Kogalym site, a hollow (H) – ridge (R) – lake complex is a dominating landscape type.

The numbers on the legend represent the following: 1, tundra; 2, forest-tundra; 3, northern taiga; 4, middle taiga; 5, borders between natural biomes; 6, borders between permafrost zones; 7, continuous permafrost; 8, discontinuous permafrost; 9, sporadic permafrost; 10, isolated permafrost; 11, key study sites with mean annual temperature in the parentheses.

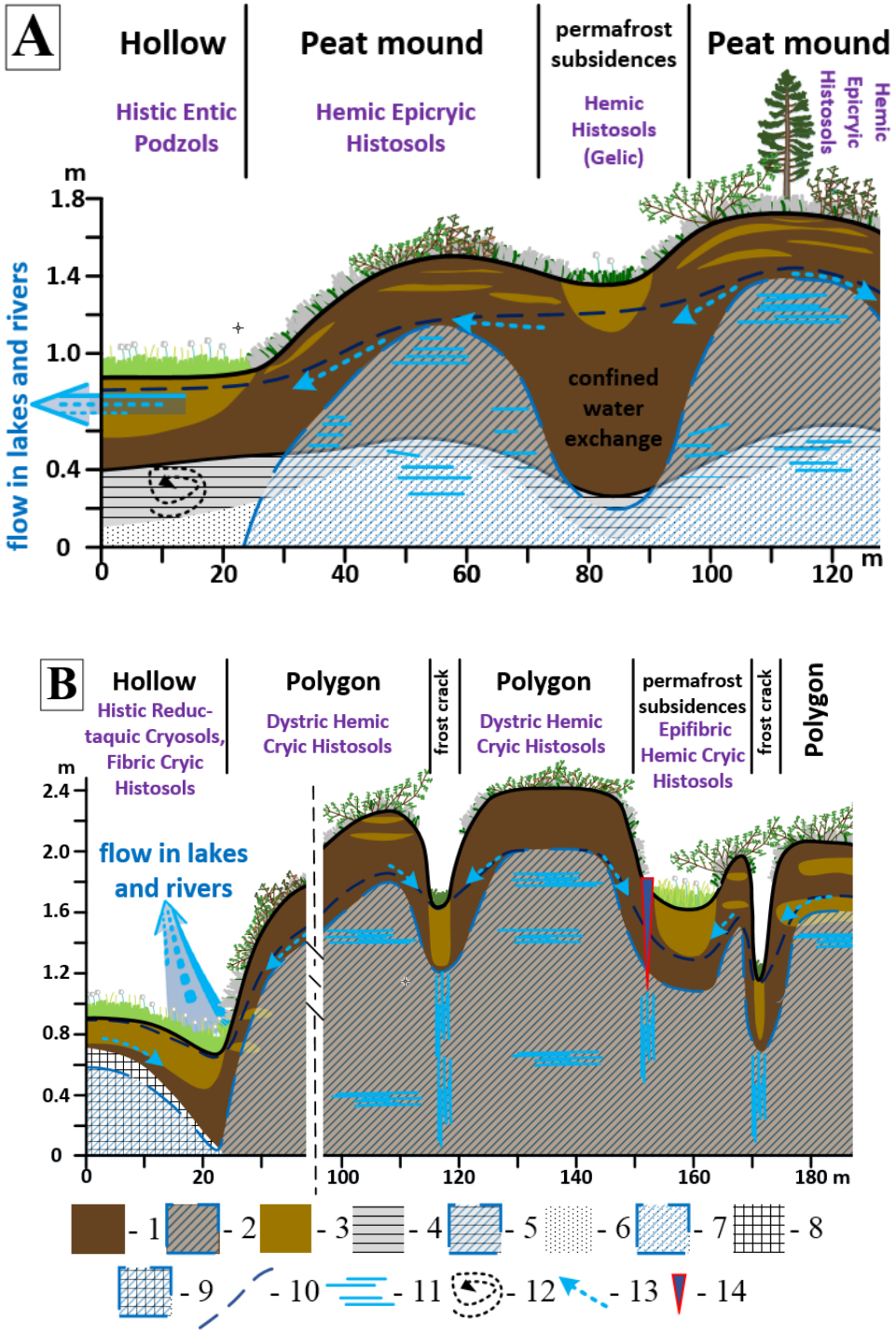


**Figure 2**. Soil transect of typical bog microlandscapes of flat mound palsa (A) and polygonal frozen bog (B). This vertical line in B indicates a discontinuity of hydrological flow-path. The numbers on the legend represent the following: 1, moss-lichen-sedge peat of medium degree of decomposition (Hemic); 2, permanently frozen peat; 3, moss-based peat of low degree of decomposition; 4, illuvial-Fe-humic (spodic) horizon; 5, permanently frozen spodic horizon; 6, sand and silt deposits; 7, frozen sand and silts; 8, heavy clay deposits; 9, frozen clays; 10, the level of suprapermafrost waters in August; 11, ice wedges; 12, cryoturbation features in soil; 13, the direction of soil water transport, typically along the permafrost boundary; 14, small crack on the polygonal bog.

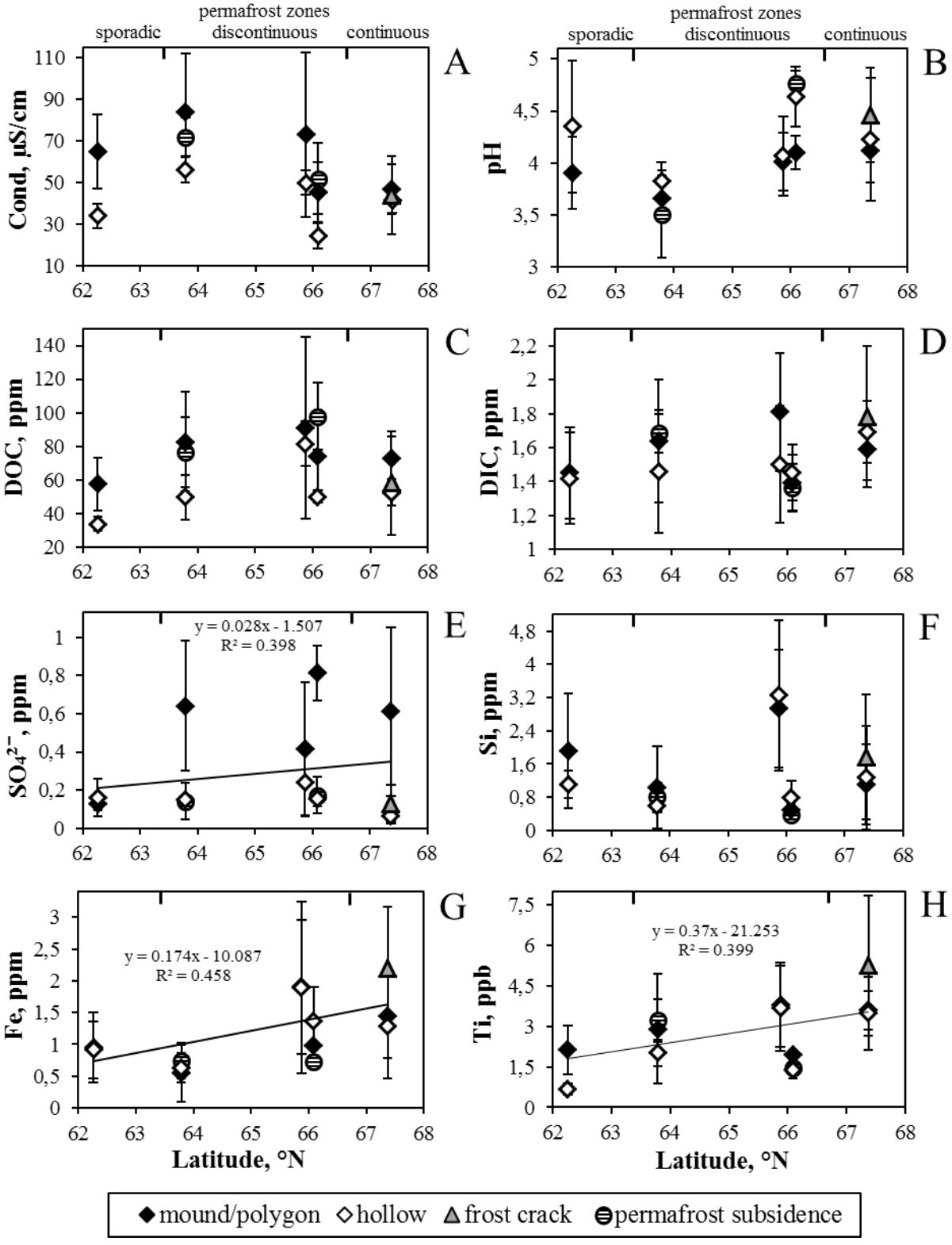


**Figure 3.** Mean values of Specific conductivity (A), pH (B), DOC (C), DIC (D), $SO_4^{2-}$ (E), Si (F), Fe (G) and Ti (H) concentration in peat porewaters of the WSL as a function of latitude for mound and polygons (solid diamonds), hollow (open diamonds), frost crack (grey triangles) and permafrost subsidence/depression (hatched circles). The solid line is a linear fit to all data with the regression equation given on each graph.

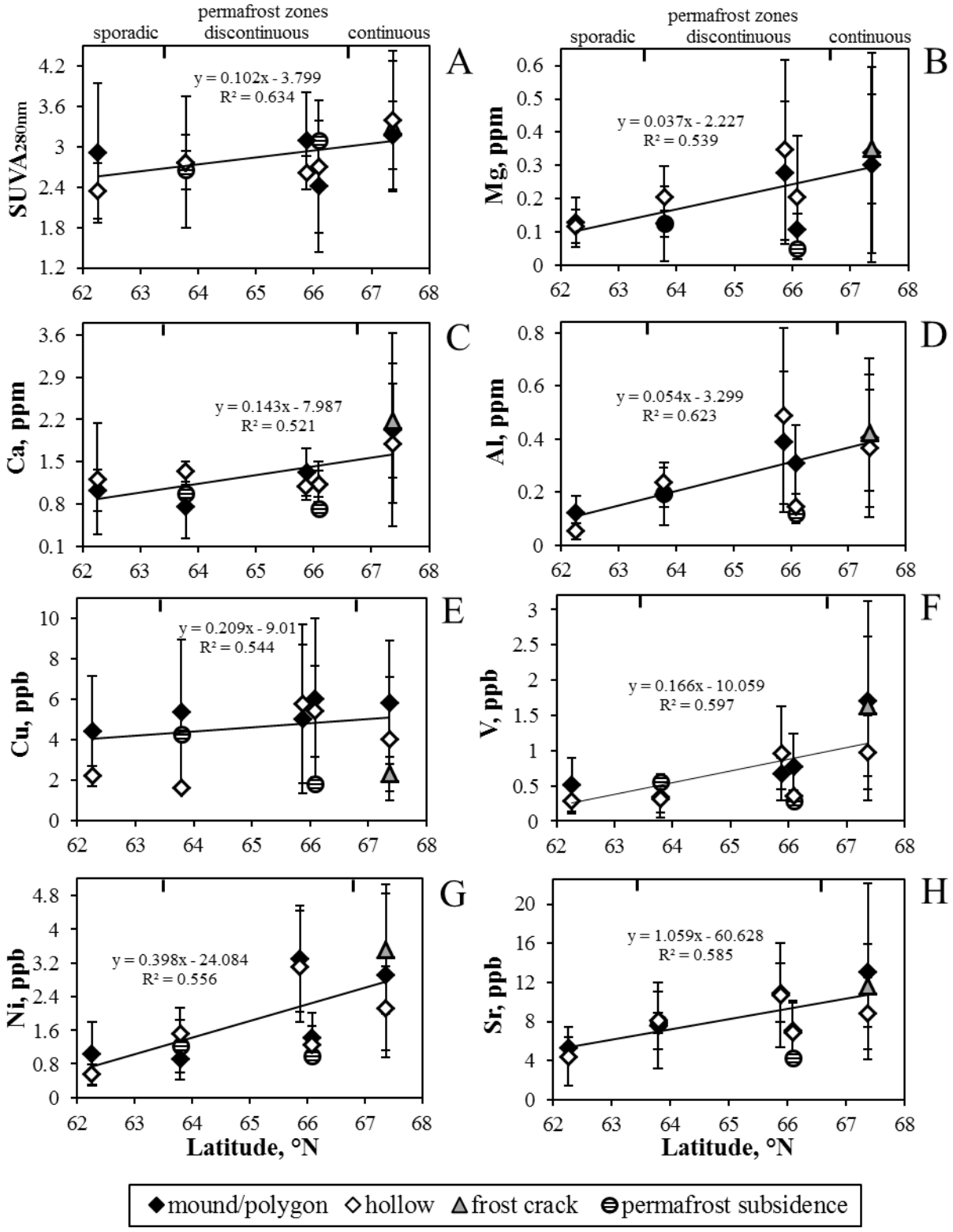


**Figure 4.** Mean values of $SUVA_{280}$ (A), Mg (B), Ca (C), Al (D), Cu (E), V (F), Ni (G), Sr (H) concentration in peat porewaters of the WSL as a function of latitude for mound and polygons (solid diamonds), hollow (open diamonds), frost crack (grey triangles) and permafrost subsidence/depression (hatched circles). The solid line is a linear fit to all data with the regression equation given on each graph.

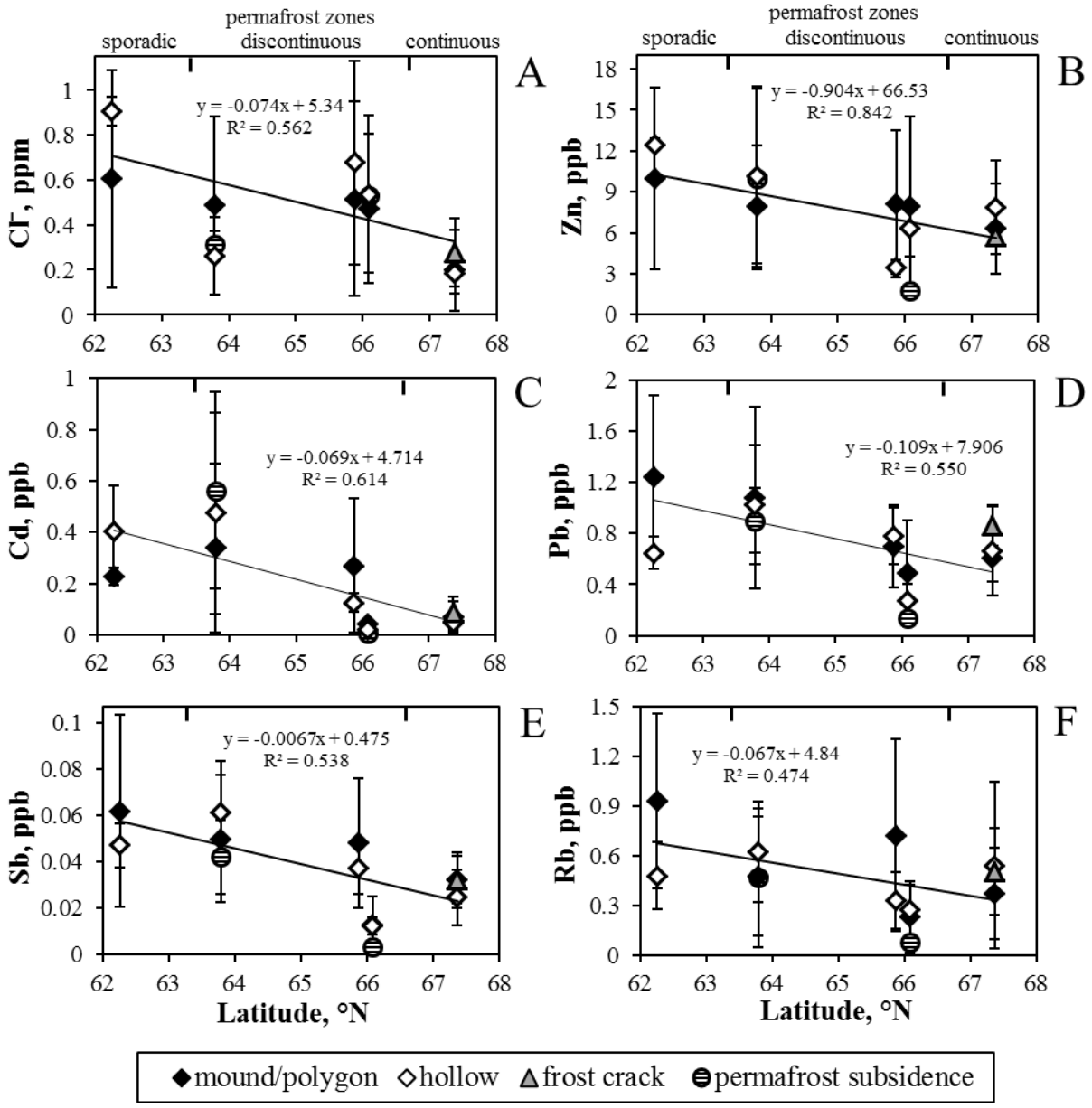


**Figure 5.** Mean concentrations of Cl (A), Zn (B), Cd (C), Pb (D), Sb (E), and Rb (F) in peat porewaters of the WSL as a function of latitude for mound and polygons (solid diamonds), hollow (open diamonds), frost crack (grey triangles) and permafrost subsidence/depression (hatched circles). The solid line is a linear fit to all data with the regression equation given on each graph.